journal of the international meteor organization

WGN

46:5
october 2018

ISSN 1016-3115

WGN Vol. 46, No. 5, October 2018, pp. 147 – 182

Administrative

Conferences

Meteor science

Preliminary results

History

Front cover photo

Fireball in Orion, captured on 2015 November 11 from Capanna Gorda, Switzerland. Photo courtesy: Ivo Scheggia.

Writing for WGN

This Journal welcomes papers submitted for publication. All papers are reviewed for scientific content, and edited for English and style. Instructions for authors can be found in WGN **45:1**, 1–5, and at `http://www.imo.net/docs/writingforwgn.pdf` .

Legal address

International Meteor Organization, Jozef Mattheessensstraat 60, 2540 Hove, Belgium.

From the Treasurer — IMO Membership/WGN Subscription Renewal for 2019

Marc Gyssens

Renewal rates

Most members/subscribers whose membership/subscription has expired should have received a reminder email. Via this way, we invite them again to renew for 2019.

The fees are as tabulated below. We are happy that we can offer WGN at the same cost in Euros as last year and that we can lower some of the US Dollar equivalents. We also continue to offer an electronic-only subscription at a reduced rate.

IMO Membership/WGN Subscription 2019				
Electronic + paper with surface mail delivery:		€26		US$ 32
Electronic + paper with airmail delivery (outside Europe only):		€49		US$ 60
Electronic only:		€21		US$ 25
Supporting membership:	add	€26	add	US$ 32

It is also possible to renew for two or more years in a row.

When you renew, give a few minutes of thought to becoming a **supporting member** by paying at least 26 EUR/32 USD extra. Smaller gifts are of course also appreciated. As you may know, there is an IMO Support Fund. With this Support Fund, we offer support to meteor-related projects. Our ability to provide this service to the meteor community depends primarily on the gifts we receive from supporting members!

Another way to help meteor workers with limited funds is to offer them a gift subscription.

We already thank all our members that will renew for their continued trust in our Organization!

Other membership benefits

The IMO Council is seeking to expand the benefits of memberships.

Last year, it was decided that the IMO's *Handbook for Meteor Observers* and *Meteor Shower Workbook* are available for free to IMO members in digital form. In this way, IMO members have at their disposal these two invaluable tools to prepare an observing session and to interpret its results. To access these publications, go to the IMO website and click on the menu item "Free Meteor Books" under the tab "Resources".

Also, International Meteor Conference (IMC) participants becoming an IMO member or renewing their IMO membership at the IMC get a reduction of 5 EUR for the next year of membership. While this measure has been taken primarily to encourage IMC participants who are not yet an IMO member to become one, established IMO members also get a small advantage each time they attend an IMC.

We intend to expand membership benefits even further in the near future.

Payment instructions

If you are not yet familiar with the new IMO website, you first must log in into your account if you want to renew. For this purpose, click the log-in button in the upper right-hand corner. As login, use the email address on which you received my reminder email. In case you forgot your password, you can use the "forgot password" link to reset it. Once logged in, you will see your profile picture (or the space provided for it). If you read on the green button below it that your membership has expired, click it, and the rest will be self-explanatory.[1]

The outcome of this process is that you will see the total amount due and your payment options. If you choose to pay using PayPal (or using a credit card via PayPal), you can complete the payment on our website.

If you experience any difficulties, do not hesitate to contact me at `treasurer@imo.net`.

One final request: every year, a lot of members renew late. As a consequence, back issues that already appeared have to be sent out to these members. Please support our volunteers in their bimonthly effort to have WGN shipped to you by renewing promptly! Thank you for your understanding and cooperation!

[1] Alternatively, you can also click on "Extend your membership" in the pull-down menu to the right of your name in the upper right-hand corner, with the same result.

Conferences

International Meteor Conference 2018 report

C. Powell[1]

Received 2018 September 30

The International Meteor Conference 2018 was held between 30th August and 2nd September in Pezinok, Slovakia, a city lying in the shadow of the Little Carpathian mountains.

Attendees travelled from all corners of the globe; those representing the Desert Fireball Network traversed half the world with 12 hour flights, whilst others such as Alan Shuttleworth took two week motorbike trips out of choice! I had a trip of many firsts: I had never flown alone before, it was my first conference, and I had never visited Slovakia before.

Figure 1 – Hotel Rozálka in Pezinok, Slovakia.

Since the age of 13, I had been interested in radio meteor detection, writing Python programs for the radio group at my local observatory. Later in my education I had the opportunity to work on a self-led research project, for which I chose to investigate temporal and spatial variation of radio data, as well as the diurnal shift phenomenon, which I then published in WGN: my first interaction with the IMO. A friend at the radio group, Alan Shuttleworth, had attended the IMC before and told me what a great experience it was. Once I started a degree in Mathematics, Emmanuel College of the University of Cambridge was able to fund my attendance at the conference, for which I am thankful and I promptly started organising my journey.

Expectations were for a formal, serious, intimidating atmosphere and consequently I felt anxious when I arrived. This feeling led me to choose not to present my research; something I now greatly regret. A warm reception desk at Hotel Rozálka welcomed participants to the conference, followed later in the evening with a short presentation by the IMO president, Cis Verbeeck, and the Local Organising Committee, who did such a fantastic job of creating IMC 2018 and presented the latest in beer-buying technology: IMC coins! The hotel provided excellent food, always starting with a hearty bowl of soup and followed by a meal that all participants will have appreciated after their journeys! As the day progressed, I felt increasingly composed and realised how wrong my premonitions were: everyone I met was friendly and eager to engage in conversation.

Figure 2 – The latest technological advancement from the IMO: IMC coins!

The first day concluded with two talks, the first a tale of searching Southern Africa for a meteorite, by Peter Jenniskens, the second an update on the European Fireball Network by Pavel Spurný, who laid down a gauntlet on clean data collection for all: these talks were a brilliant introduction to the conference; a formal occasion for the presentation of science, yet also a relaxing atmosphere for discussion. Being able to talk about my own research projects with others was extremely helpful and has greatly enhanced my ideas: opportunities such as these are why conferences are so fantastic!

[1] Email: cpowell@cwp.io

IMO bibcode WGN-465-powell-imc2018 NASA-ADS bibcode 2018JIMO...46..148P

An intensive schedule ensured everyone was busy on the first full day, with talks from 9am to 6pm and frequent interludes to refuel with coffee and discuss the talks. During these breaks, participants had the opportunity to view the 25 posters, all of excellent quality and demonstrating the capability of amateur science.

Figure 3 – Lecture theatre where talks were held and posters could be viewed.

The wide variety of topics in the talks should be applauded, ranging from video meteor detection using balloons: the MALBEC project (J. Vaubaillon, A. Caillou), to measurements of the Population Index with cameras (P. Slansky). Felix Bettonvil even demonstrated that meteor science provides an excellent excuse to make a cannon. The conference also exhibited the breadth of possible involvement in meteor detection, with setups costing very little using Raspberry Pi's, to pricetags that startle many with the Desert Fireball Network's observation setup.

The day ended with the IMO General Assembly meeting, where Cis and Marc Gyssens gave an update on the status of the IMO. To summarise briefly, everything's going well! Jürgen Rendtel proposed the IMC 2019 venue in Germany, near Potsdam – I won't give too much away. Both Jürgen and Cis emphasised the need for future IMCs to be proposed, so please do! After every day my mind was frazzled, though especially after such a long day of talks.

The second full day started with a morning of further talks, followed by the excursion. This year, participants visited the Red Stone castle near Modra, where we were led on tours of the Renaissance-Baroque castle dating back to the 16th century, which offers an insight into the historical lives of the noble families of Slovakia.

Figure 4 – IMC participants exploring the red stone castle.

Upon returning to the coaches to travel to the AGO Observatory, the heavens opened and we could not visit the observatory, and instead returned to the conference venue amid cracks of thunder to discuss the past days of talks. After a conference dinner, participants were treated to a traditional Slovakian folklore performance which later required crowd involvement! Beer started flowing and subsequently the traditional IMC song was sung – Jeremie put down his guitar this year and another took up the duty.

On the penultimate day of the conference, the WGN editor-in-chief Javor asked me if I would like to write this report, as a first-time attendee of the IMC, for which I am thankful. I leaped at the chance, as I now have the opportunity to express my thanks to the organisers, presenters, poster-creators, scientists, and all involved, as well as commenting on the impact of the conference on me. After a final morning of talks, including a plea for data (yes, even more data) by Galina Ryabova, the conference ended and participants departed. I was sad to leave the conference as it had been a truly eye-opening experience: everyone I met left an impression on me, many of the talks captivated me, and the connections formed reach far further than I could have imagined.

Figure 5 – Traditional Slovakian folklore performance.

The greatest influence of the International Meteor Organisation is communication; from which science thrives. To bring scientists, amateur, professional, or simply enthusiastic, from all around the world is an incredible feat.

The local organising committee organised the conference to the utmost standard: infinite thanks is due to all of them. Equally, the quality of presentations and posters was exceptional. The scientific content available bred many discussions and no doubt inspired many future projects and ideas.

Upon arrival, I was anxious. Upon departure, I felt like I had become an integrated member of the IMO community – a community I hope to remain in for many years to come. Days passed before I fully processed how I felt.

I look forward to meeting everyone again at IMC 2019, and wish clear skies and clean data to all!

Figure 6 – Participants of IMC 2018.

IMC 2019 October 3–6 in Germany

Jürgen Rendtel[1]

Every three years, there is the chance to organise the IMC in conjunction with the "Meteoroids" conference. This worked well on several occasions, and it was also tried for 2019 when the "Meteoroids" takes place in Bratislava in June. However, this plan in various modifications did not work out.

Once it became clear that the double conference arrangement will not be possible, the German meteor observers contacted the KIEZ Bollmannsruh near the city of Brandenburg (Havel) which was already the IMC venue in 2003. The location is not too far from Berlin, and they made an affordable offer which allowed us to book the entire campus for the IMC after the main season. The city of Brandenburg can be easily reached from the nearby airports by public transport and by car. So the IMO Council decided to have the IMC 2019 in Bollmannsruh.

The Local Organising Committee consists of Rainer Arlt, André Knöfel, Sirko Molau, Ina Rendtel, Jürgen Rendtel and Roland Winkler. Further details will be given in the next issue of WGN and on the web pages in due time. So mark your calendar: after 16 years back again to Bollmannsruh, Germany, for the IMC 2019 October 3–6. We look forward to see you there.

[1] Leibniz-Institut für Astrophysik Potsdam (AIP) An der Sternwarte 16, 14482 Potsdam, Germany. jrendtel@aip.de

Meteor science

Multi-Year Observations of Geminid Meteor Showers with GRT-WF

Ken Watanabe[1] *and Martin B. Marks*[1]

We observed the Geminid meteor shower returns 2011-2017 using the Goddard Robotic Telescope Wide Field (GRT-WF) located at the Florida Guld Coast University campus in Fort Myers, Florida, USA. The instrument was originally designed to observe SPRITEs to study possible connections between SPRITEs and Terrestrial Gamma-ray Flashes (TGFs). However, we were able to utilize it to derive the population index (r) and the Zenithal Hourly Rate (ZHR) as a function of solar longitude (2000.0) as well as the variation of ZHR during the period.

Received 2018 August 6

1 Introduction

The Goddard Robotic Telescope Wide Field (GRT-WF, Figure 1) is a sister instrument of the Goddard Robotic Telescope (GRT; Sakamoto et al., 2011), funded by NASA Grant [a], located at Florida Gulf Coast University (FGCU), Fort Myers, Florida. The GRT-WF consists of seven Watec 902H2 Ultimate CCD cameras with Fujinon YV2.7x2.9LR4D-SA2 lenses ($f/D = 0.95$). Each camera is connected to a PC using Dazzle DVD Recorder Plus to convert a video signal to a digital one. UFOCaptureV2 (Sonotaco.com) software is utilized to record images of sprites, meteors, and lightnings. The operation started in June 2011 to primarily study possible correlations between sprites and TGFs (Terrestrial Gamma-ray Flashes).

Its field of view is roughly $40° \times 60°$ for each camera. Therefore, the system covers the entire sky except the zenith region (see Figure 2).

The recording frame rate is 30 per second, and the image capture time duration is from $T - 1$ seconds to $T + 2$ seconds. The image sensitivity in a single frame allows us to detect meteors up to about +3 magnitude. The reason of exclusion of the zenith region is that we cannot see any sprites occurring just above us because we are always covered by the storm clouds at that time epoch. Thus, this instrument is not ideal for meteor shower observations.

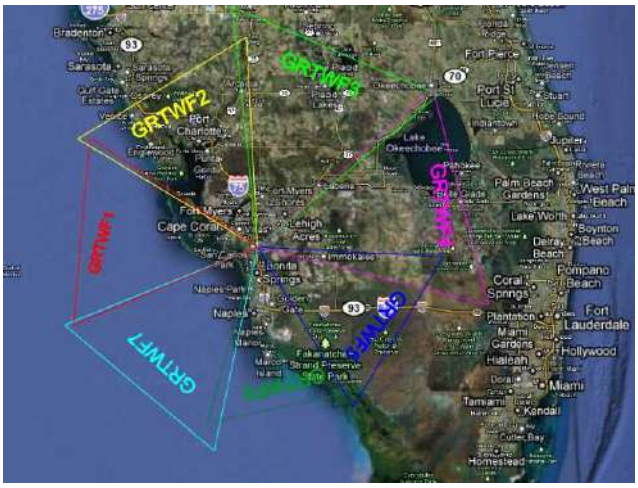

Figure 2 – Directions of the GRT-WF cameras.

[1]Department of Chemistry and Physics, College of Arts and Science, Florida Gulf Coast University, Fort Myers, FL, 33965-6565, USA. Email: kwatanab@fgcu.edu

IMO bibcode WGN-465-watanabe-geminids
NASA-ADS bibcode 2018JIMO...46..151W

[a]NASA Research Announcement NNH09ZDA001N

Figure 1 – GRT-WF located on FGCU campus in Fort Myers, Florida, USA.

2 Data from GRT-WF

We retrieved data from the Geminid returns between 2011 and 2017 (except 2014) detected by GR-WF with UFO Analyzer V2 (Sonotaco.com), and divided them into sub-groups with a two-hour time bin (see Table 1). No data were available in 2014 due to system downtime. Cameras 4 and 7 never detected any Geminids due to technical difficulties. Camera 2 was the only one which was functioning in 2017 because we were still recovering damages from Hurricane Irma.

The elevation angle of the radiant around the peak is relatively high ($> 70°$). The radiant elevation exceeds $70°$ during some time of the night.

We find that many detected meteors are bright (magnitude up to -4). When excluding the field around the zenith, we probably miss a significant amount of meteors close to the radiant which may include a large fraction of faint meteors.

Table 1 – Geminid data per year observed by GRT-WF There were no data available in 2014 due to technical diffi culties.

Year	Number of Geminids	Observed Time (h)	Cameras
2011	109	8	1,2,3
2012	55	4	1,2,3,5,6
2013	213	12	1,2,3,5,6
2014	0	0	
2015	81	4	1,2,3,5,6
2016	99	12	2,3,6
2017	99	7.5	2

3 Data Analysis

We followed the standard procedure described by Brown and Rendtel (1996) to drive the population index and the ZHR as a function of Solar Longitude (2000.0).

Starting with Equation (5) of Brown and Rendtel (1996), meteor brightness (M_v) can be expressed as

$$M_v = \frac{\log_{10}[N_c(M_v)]}{\log_{10}(r)} - \frac{\log_{10} K}{\log_{10}(r)} \quad (1)$$

where $N_c(M_v)$ is the true cumulative number of meteors brighter than M_v, r is the population index, and K is a constant multiplier as explained by Brown and Rendtel (1996).

We linearly fitted the M_v vs. $\log_{10}[N_c(M_v)]$ graph to derive the slope (m) of the function of (1) and the standard deviation of m, σ_m. Since

$$m = \frac{1}{\log_{10}(r)} \quad (2)$$

and the standard deviation of r, σ_r, is related with σ_m as

$$\sigma_m = \left(\frac{\partial m}{\partial r}\right)\sigma_r \quad (3)$$

After a little mathematical manipulation, one can find that the standard deviation of r, σ_r, is calculated as

$$\sigma_r = \frac{-r(\ln r)^2}{\ln 10}\sigma_m \quad (4)$$

Equation (1) of Brown and Rendtel (1996) defines the ZHR. We can calculate the standard deviation of the ZHR as

$$\sigma_{\mathrm{ZHR}} = \left(\frac{\partial \mathrm{ZHR}}{\partial r}\right) = \frac{6.5 - \mathrm{LM} N r^{6.5-\mathrm{LM}}}{\sin h_R T_{\mathrm{eff}}} \quad (5)$$

where LM is the limiting magnitude, N is the number of meteors observed during the effective observation time T_{eff} and h_R is the radiant elevation.

Since GRT-WF is considered a single observer, we are not able to compute the statistical errors obtained from multiple observers. We, instead, use the theoretical standard deviations stated above in our presentations. Therefore, the errors in r and ZHR are generally larger than those statistically calculated from multiple observers.

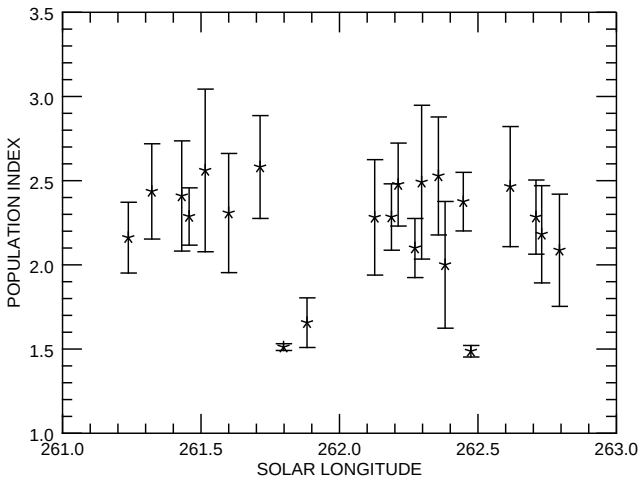

Figure 3 – Variation of the population index function of the Solar Longitude $\lambda_\odot$.

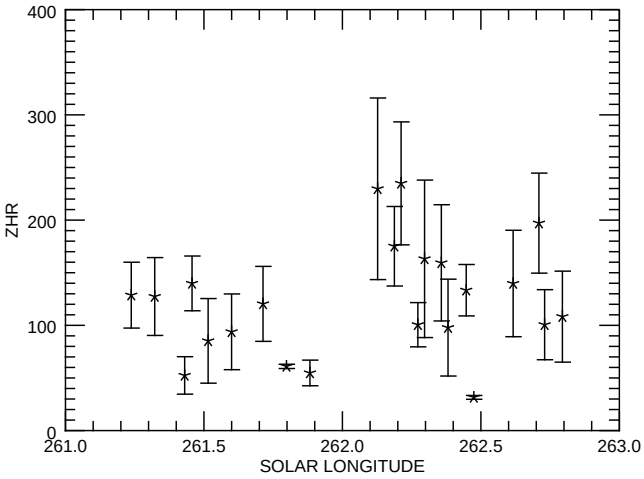

Figure 4 – ZHR profile of the Geminids 2011–2014.

4 Results and Discussion

Figure 3 shows the population index r as a function of the solar longitude (2000.0) derived from our data study. Although, as explained in the previous section, the error bars based on $1\sigma_r$ are slightly larger (the average is 0.31) than those of Rendtel (2004) for 1991–2001, the overall r values are similar. Rendtel (2004) pointed out that there are minima at $\lambda_\odot = 261\overset{\circ}{.}92 \pm 0\overset{\circ}{.}03$ ($r = 2.18 \pm 0.12$), $\lambda_\odot = 262\overset{\circ}{.}12 \pm 0\overset{\circ}{.}05$ ($r = 1.92 \pm 0.04$), and $\lambda_\odot = 262\overset{\circ}{.}4$Âś$0\overset{\circ}{.}06$ ($r = 1.75 \pm 0.06$). We also found the local minima at $\lambda_\odot = 261\overset{\circ}{.}8 \pm 0\overset{\circ}{.}04$ ($r = 1.51 \pm 0.02$) and $262\overset{\circ}{.}47 \pm 0\overset{\circ}{.}04$ ($r = 1.48 \pm 0.03$), but not around at $\lambda_\odot = 262\overset{\circ}{.}12$.

Although the fitted slopes of Equation (1) for these two points are steeper than any other points, their uncertainties are relatively small. Because the absolute values of the population index error margins are directly proportional to these small numbers (see Equation (4)), the error margins are also small. Other error bars could have been smaller if we had more samples.

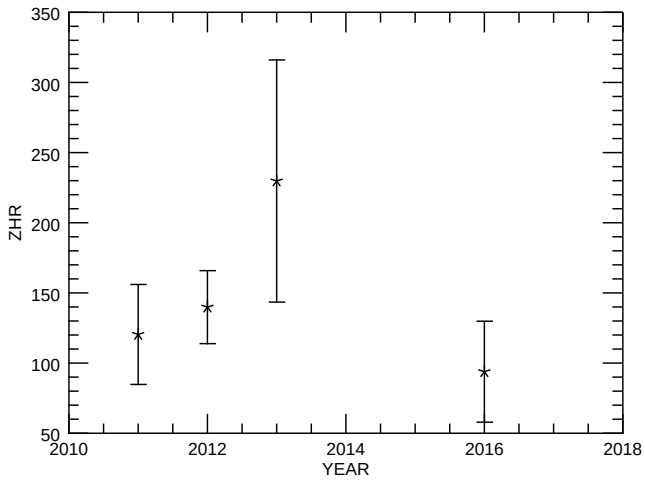

Figure 5 – Peak values of the ZHR at $\lambda_\odot = 261^\circ - 262^\circ$ in each year.

We set $\gamma = 1$ for Equation (1) of Brown and Rendtel (1996) to calculate ZHR because the radiant is always larger than 20° altitude in our observations. Figure 4 illustrates variations of ZHR in function of the solar longitude (2000.0) from all observed returns. The two 200+ values appear consecutively during the same night in 2013 which also shows the highest ZHRs in Figure 5. The numbers of both samples are fairly large as compared to other ones. However, we do not yet understand why the ZHRs are much larger than the other values.

We are not able to derive fine structures of the ZHR variations as found by Rendtel (2004) due to the relatively small number of samples available to us.

For the Leonids, Arlt (2003) reported a decreasing r with increasing radiant elevation while Bellot-Rubio (1995) indicated an increase of r, instead. Our observations with Geminid do not show any r dependencies of radiant elevation.

Ryabova and Rendtel (2018) reported that the Geminid meteor shower activity is increasing in time based on observations between 1985 and 2016. Figure 5, which shows the peak ZHR in 2011, 2012, 2013, and 2016 in the period $\lambda_\odot = 261^\circ - 262^\circ$ from this study, also indicates the trend of increase in the first three years of our observations. The lower ZHR in 2016 could be just a fluctuation, a dip or the begin of a reverse trend. For 2017, we did not add a value since the sample consist only of data from one camera.

5 Conclusions

We observed the Geminid meteor shower from 2011 to 2017, except 2014, using the GRT-WF located in Fort Myers, Florida. The purpose of this work is to show that GRT-WF data can be used for meteor shower analysis. We derived the population index r and the ZHR as a function of the solar longitude. We found the local minima of r similar to those previously reported by Rendtel (2004). Our error margins are based on the theoretical standard deviations from fitting equation (1), and they tend to be larger than those statistically obtained from multiple observers. Next we will work on recently obtained Perseid data, applying the same method as used here. We also plan to continue observing the Geminids.

References

Arlt R. (2003). "Bulletin 19 of the International Leonid Watch: Population index study of the 2002 Leonid meteors". *WGN, Journal of the IMO*, **31**, 77–87.

Bellot Rubio L. R. (1995). "Effects of a dependence of meteor brightness on the entry angle". *Astron. Astrophys.*, **301**, 602–608.

Brown P. and Rendtel J. (1996). "The Perseid Meteoroid Stream: Characterization of Recent Activity from Visual Observations". *Icarus*, **124**, 414–428.

Rendtel J. (2004). "Evolution of the Geminids Observed Over 60 Years". *Earth, Moon and Planets*, **95**, 27–32.

Ryabova G. O. and Rendtel J. (2018). "Increasing Geminid meteor shower activity". *MNRAS*, **475**, 77–80.

Sakamoto T., Wallace C. A., Donato D., Gehrels N., Okajima T., and Ukwatta T. N. (2011). "Goddard Robotic Telescope - Optical follow-up of GRBs and coordinated observations of AGNs". *Adv. Space Res.*, pages 1444–1450.

Handling Editor: Jürgen Rendtel

Correction for meteor centroids observed using rolling shutter cameras

Patrik Kukić[1], *Peter Gural*[2], *Denis Vida*[3,4], *Damir Šegon*[5], *and Aleksandar Merlak*[6]

As the currently prevalent analog CCD sensors used in meteor cameras are being phased out by manufacturers, amateur meteor astronomers have been investigating the use of low-cost CMOS alternatives. Many CMOS cameras in the lower price range (<100 USD) have a top-to-bottom, sequentially delayed exposure start time (rolling shutter) which can influence meteor centroids and subsequently the estimation of meteor dynamics. Here we present two methods, one temporal and one spatial, of correcting for the rolling shutter effect and demonstrate the correction in practice. The code used to demonstrate the effects and corrections is available on GitHub (`https://github.com/PKukic/RollingShutterSim`). We show that the rolling shutter effect, although minor for moderate field of view meteor video systems, can be corrected for and that the correction residuals are within the image centroid measurement accuracy.

Received 2018 July 25

1 Introduction

Currently prevalent CCD sensors, that are used in video meteor cameras, are starting to be phased out. In 2015 Sony announced they would discontinue manufacturing all CCD sensors by 2020 and completely focus on CMOS technology. Since most meteor networks use analog video cameras with Sony CCD sensors (Brown et al., 2010; Jenniskens et al., 2011; Samuels et al., 2014), the announcement has a significant impact on the meteor community.

In the domain of progressive scan CMOS sensors, all circa 2018 low-cost sensors (<100 USD) have rolling shutters, while only the more expensive cameras use a global shutter technology (e.g. the Sony Pregius line of CMOS cameras). A CMOS global shutter behaves like a CCD sensor, in that each pixel starts and stops its exposure at the same time. In rolling shutter cameras, each sensor row of pixels starts their exposure a fixed delay after the previous row's pixels (temporal delay of $1/(n_{rows} \times FPS)$, e.g. in the case of a 720p camera operated at 25 FPS the time delay is 56 µs), thus each pixel row represents a different time window. The exposure for each row stops a fixed integration time after the start, which can vary from a few microseconds to as high as the frame-to-frame time (1/FPS) of the sensor. The rolling shutter exposure delays per row distorts fast-moving objects, since each pixel row has captured the moving object at a different time and spatial position. In global shutter cameras, since all pixels start and stop their integration simultaneously, they are effectively taking a snapshot of the object at a single instant in time. Most of the previously used analog CCD cameras had interlaced video which influenced meteor centroids in a different way due to alternating missing rows. But they in fact offered double the temporal resolution by sacrificing half the vertical resolution (e.g. 50 half frames (fields) per second instead of 25 frames per second) (Vida et al., 2016). Progressive scan CMOS sensors do not use interlacing thus avoiding missing rows in the centroid estimate. Figure 1 illustrates the difference between various exposure methods of global shutter, interlaced, and rolling shutter. It should be noted that the reason for the rolling shutter design resides in the simple and efficient approach to sequentially read each row in a time delayed fashion.

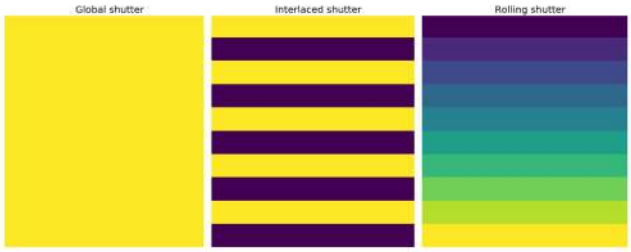

Figure 1 – Left: Global shutters read out the whole image at once at $1/FPS$ intervals. Middle: The reading of alternating odd and even rows in interlaced video occurs in $1/(2 \times FPS)$ intervals. Right: Every row in the rolling shutter is exposed and read out sequentially, $1/(n_{rows} \times FPS)$ seconds after the other.

The centroid of a meteor streak captured by a rolling shutter camera will shift relative to the global shutter centroid along the meteor's direction of motion, which is dependent on angle and apparent angular velocity on the focal plane. Horizontal meteors have no centroid shift because the "reader" (the leading edge of pixel integration) meets the meteor in regular time intervals of $1/FPS$, while centroids of vertical meteors are affected the most because the reader meets them at constantly changing time intervals. Note that this effect is similar to the effect of a mechanical rotating shutter used by photographic fireball networks in the past, which also had to be corrected for (Ceplecha, 1987).

It should be noted that rolling shutter is even more distorting if the camera is slewing or jittering as in a hand held cell phone video. It will appear to look like viewing through "jello" and involves more sophisticated corrections than we present here for a fixed mounted meteor camera. For meteors, the rolling shutter impacts the vertical spread of the meteor, stretching the meteor

[1]XV Gymnasium, Jordanovac 8, HR-10000 Zagreb, Croatia
[2]Gural Software Development
[3]Department of Earth Sciences, University of Western Ontario, London, Ontario, N6A 5B7, Canada
[4]Department of Physics and Astronomy, University of Western Ontario, London, Ontario, N6A 3K7, Canada
[5]Astronomical Society Istra Pula, Park Monte Zaro 2, HR-52100 Pula, Croatia
[6]ISTRA STREAM d.o.o., Hum, Croatia

IMO bibcode WGN-465-kukic-rolling
NASA-ADS bibcode 2018JIMO...46..154K

streak when it moves downward, fore-shortening when it moves upwards, with a bias in the direction of motion.

In this paper we investigate rolling shutter effects on meteor centroids by creating synthetic meteor videos and simulating the rolling shutter effect. We develop two methods of centroid correction (temporal and spatial) and demonstrate that both produce corrected centroids which are within the centroid measurement uncertainty. The corrections can account for the integration time being less than the frame-to-frame time.

2 Methods

2.1 Simulating meteors and rolling shutter effects

In this section we discuss details of the meteor simulation. Two independent simulations were developed to validate results, but only one will be described herein. The meteor was represented as a propagating streak along a line that passed through the centre of the image. The duration of the meteor was estimated using the apparent angular velocity of the meteor ω (in units of '/s) and a pixel scale k (in units of '/px). A square-pixel, non-warped image scale was calculated by dividing one dimension of the field of view (FOV) in degrees with one dimension of the image resolution:

$$k = (60'/^\circ)\frac{\theta_h}{X_{size}} \approx (60'/^\circ)\frac{\theta_v}{n_{rows}} \quad (1)$$

where θ_h and θ_v are horizontal and vertical sizes of the FOV in degrees, while X_{size} and n_{rows} are the horizontal and the vertical image resolution, respectively. We modeled a camera with the resolution of 1280×720, a FOV of $42^\circ \times 24^\circ$, which corresponds to a 6 mm $f/1.2$ lens. This gave a pixel scale of $k \approx 2$ '/px. To simulate the effect of meteor deceleration, the meteor's angular velocity at a given point in time was computed using the empirical exponential deceleration model by Jacchia & Whipple (1961):

$$\omega(t) = \omega_0 - ab\exp(bt) \quad (2)$$

where ω_0 is the initial angular velocity of the meteor, measured in '/s, and a ['] and $b[\mathrm{s}^{-1}]$ are the deceleration coefficients. In the case of a constant velocity meteor, a or b are 0. Given the difference between the initial angular velocity ω_0 and a final angular velocity $\omega(t)$, deceleration parameters can be computed. Rearranging the equation (2) gives the following expression:

$$\Delta\omega = \omega_0 - \omega(t) = ab\exp(bt) \quad (3)$$

If we keep a fixed, b can be found using the following equation:

$$b = \frac{\Re\left(W\left(\frac{t}{a}\left(\omega_0 - \omega(t)\right)\right)\right)}{t} \quad (4)$$

where $\Re$ denotes the real part of the Lambert-W function. Several deceleration profiles based on various velocity differences ($\Delta\omega$) are shown in Figure 2 (the a parameter was fixed at 0.06', and the b parameter was computed). In all our simulations we have assumed that the meteor will decelerate 10% from its initial velocity.

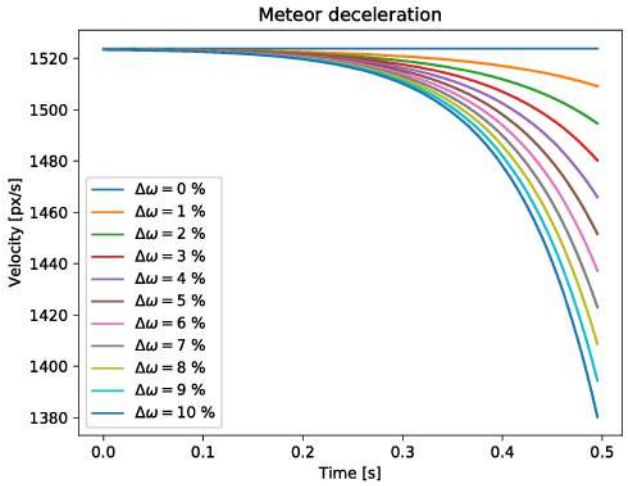

Figure 2 – Several exponential deceleration profiles based on different velocity losses. The velocity loss is expressed as a percentage of the initial meteor velocity.

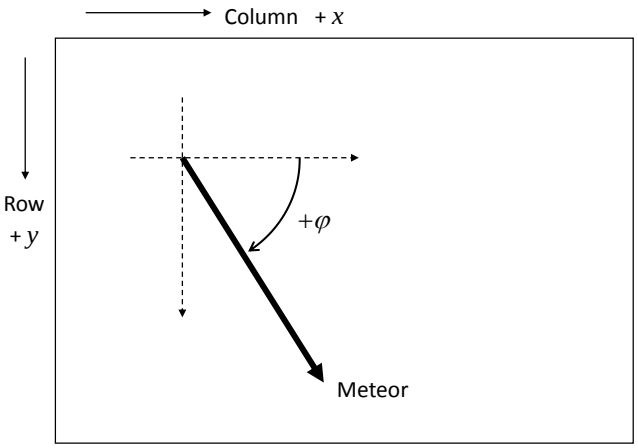

Figure 3 – The image coordinate system.

Next, the distance from the image centre at time t, $R(t)$ is calculated as:

$$R(t) = \frac{\omega(t)t}{k} \quad (5)$$

The coordinates of the points on the line are transformed from polar to Cartesian image coordinates (x, y) using the following equations:

$$\begin{aligned} x &= x_{center} + R\cos\varphi \\ y &= y_{center} + R\sin\varphi \end{aligned} \quad (6)$$

where x_{center} and y_{center} are the coordinates of the image centre and φ is the angle of the meteor from the horizontal, measured positive clockwise. Note that the origin of this system is in the upper left-hand corner of the image, and that the Y axis has been inverted. Figure 3 illustrates the coordinate system.

The total number of frames is computed as a ratio of the duration of the meteor and frames per second (FPS). In our simulation we used the FPS of 25. The

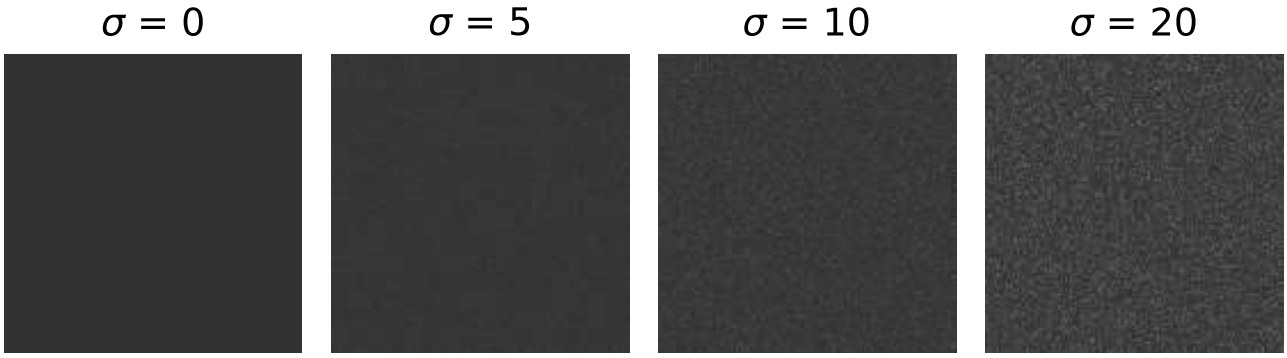

Figure 4 – From left to right: Background noise levels of 0, 5, 10 and 20.

duration is computed from the angle and meteor's angular speed, making sure the computed positions are always within the image. We considered every computed position of the meteor as a light source approximated by a Gaussian point spread function (PSF) which was evaluated and added to the simulated video frame matrix. The following formulation of a two-dimensional Gaussian function was used:

$$f(x,y) = A\exp\left(-\left(\frac{(x-x_0)^2}{2\sigma_x^2}+\frac{(y-y_0)^2}{2\sigma_y^2}\right)\right) \quad (7)$$

where A is the amplitude which we keep at unity, (x_0, y_0) are the coordinates of the centre of the Gaussian, and σ_x and σ_y are standard deviations along the respective axes. To speed up the computation, we only evaluate the Gaussian within a 3σ window from its centre, as any values outside that window are effectively 0. We used the values of standard deviations of $\sigma_x = \sigma_y = 2$ px. To simulate the meteor trail, we compute the position of the meteor on hundreds of fine spatial steps between the beginning and the end of the frame, evaluate the PSF to every point and integrate them.

After the simulated frame integration was done, Gaussian noise was added to the image to simulate the readout noise. The intensity integration was performed using a floating point matrix. We scaled the peak intensity of the image to 255 and converted the image to an 8-bit unsigned integer to simulate the digitization process. This way we made sure all simulated meteors are of the same brightness regardless of speed and also prevented saturation effects.

Finally, the simulated frame was generated by reading out the sensor image matrix via either a global or a rolling shutter. When reading out the image with a global shutter, the whole sensor image was read out at once, hence the read out frame was equal to the sensor image matrix. When reading out the sensor image matrix with a rolling shutter, the following method was used: the first frame of the meteor was used as an initialization frame, thus ensuring all rows have equal exposure time. The readout started with the second frame, where the image rows were read out top to bottom with a temporal shift of $1/(720\times 25) = 55$ µs after the sensor image matrix was updated for that temporal shift. Immediately after a specific row was read out, the values in that same row of the sensor image matrix were reset to 0.

The coordinates of the meteor on each simulated frame were computed by centroiding the meteor streak. The centroid in the X dimension was computed as:

$$x_{centroid} = \frac{\sum_{x=0}^{N}\sum_{y=0}^{M} x\left(I_{x,y}-I_{noise}\right)}{\sum_{x=0}^{N}\sum_{y=0}^{M}\left(I_{x,y}-I_{noise}\right)} \quad (8)$$

where (N, M) is the size of the centroiding window (we only centroided everything inside 3σ from the extreme points on the meteor track), $I_{x,y}$ is the pixel intensity at position x, y) and I_{noise} is the background noise intensity. The background noise intensity is estimated as the mean value of all pixel intensities outside the meteor window. This same approach was used to find the centroid in the Y dimension with the numerator term x replaced by y.

After developing the simulation, it was tested by generating multiple meteors with their velocities ranging from 5 to 50°/s (a range of meteor angular velocities one might observe on the sky), while their angle was fixed at a value of 45°. For a scale of 2 '/px, the on-chip meteor velocities were thus in the range of 150 to 1500 px/s. The influence of four different levels of background noise on centroid estimation was performed by adding Gaussian noise with standard deviations of: 0 (no noise), 5, 10, and 20 to the imagery. Figure 4 shows a sample of every simulated background noise level.

We computed the centroids from the images with different background noise levels and compared them to the known modeled centroid values. The results are shown in Figure 5. The centroid offset (that is, the distance between the real and computed centroid point) was under 0.2 pixels even with the highest modeled noise level. Please note that these are the best case centroid values as we used the highest signal-to-noise ratio of an sensor with 8 bit dynamic range (all meteor peaks were at the level of 255), the real-world values may be worse. We show similar graphs later in the paper for corrected centroids to demonstrate the feasibility of the proposed correction methods in the presence of noise.
Next was an investigation on the influence of a simulated rolling shutter on meteor centroids, by simulating several meteors with various angles and angular veloci-

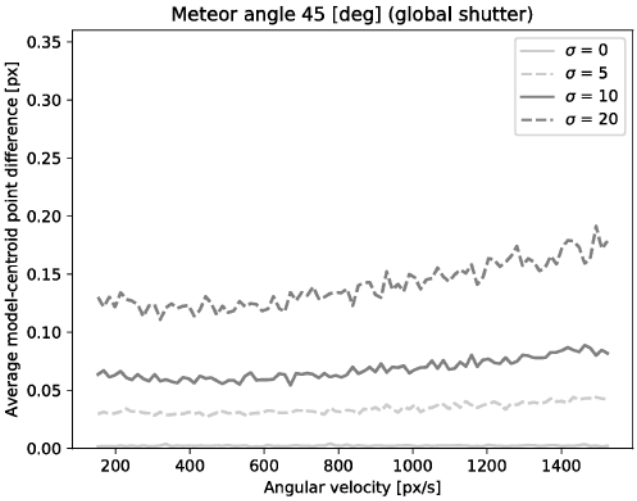

Figure 5 – Theoretical ideal centroid precision, depending on meteor velocity and noise level.

ties. We noted that when captured by a rolling shutter, the meteor centroids moved relative to the true centroid along the direction of the motion of the meteor. One example is shown in Figure 6. The simulated meteor was moving from upper left to lower right. In the top half of the image, the centroids are behind the true (model) position in the direction of motion, (they are behind the center of the global shutter gray streak), at approximately half the image height in pixels the centroid is located close to the center of the global track, and at the bottom half the rolling shutter centroid is now leading the true mean position of the meteor. The consequences of this behavior is that the velocity estimate from a rolling shutter will be larger than for the same meteor seen from a global shutter! If the meteor were moving upwards, the velocity would appear to be smaller for rolling versus global.

Next, we repeated the analysis of centroids and noise levels, but this time with the rolling shutter effect included. In contrast to the results obtained in the global shutter simulations, the maximum centroid offset was just under 30 pixels and its value was proportional to the meteor's on-chip velocity, as shown in Figure 7. Note that all noise levels on the figure are all on top of one another as the rolling shutter effect dominates the centroid difference for the plot scale used.

These results show that the rolling shutter significantly influences positions of centroids along the direction of the meteor's motion for meteors with a high apparent velocity, and that a correction is needed to have accurate centroid coordinates and thus correct velocity estimation. The relationship between the meteor's angle, the centroid's Y coordinate and the centroid offset was also investigated. A meteor was simulated for each angle from 0° to 360°, while its velocity was fixed at a high value of 1500 px/s, the results are shown in Figure 8. We noticed that the meteor angle does not influence the direction of the centroid offset – they are distributed along the line on the plot. Instead, the amount of centroid offset was found to be inversely proportional to the Y coordinate of the meteor centroid.

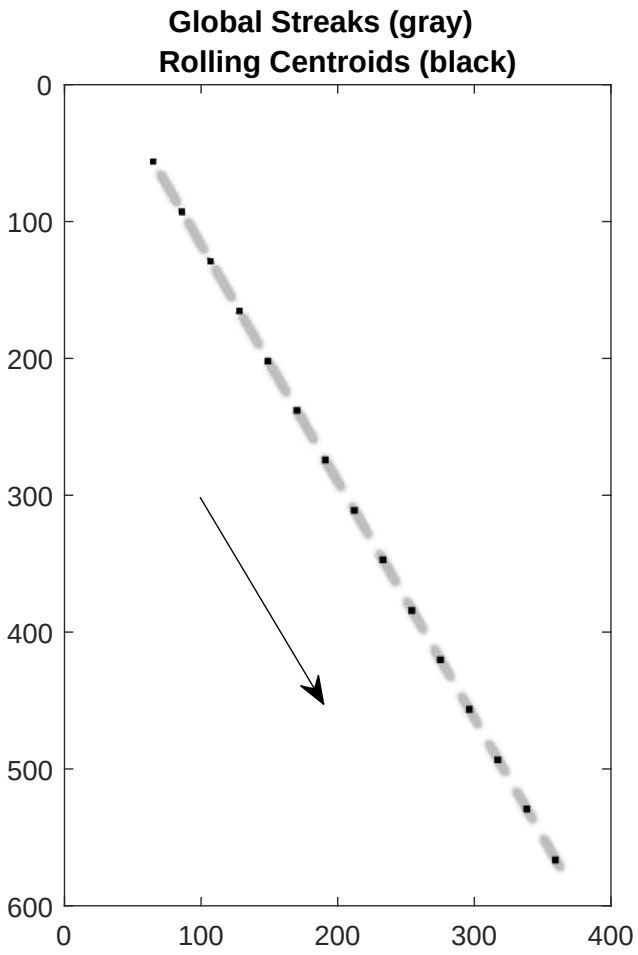

Figure 6 – Rolling shutter centroids changing position relative to the center of global shutter tracks.

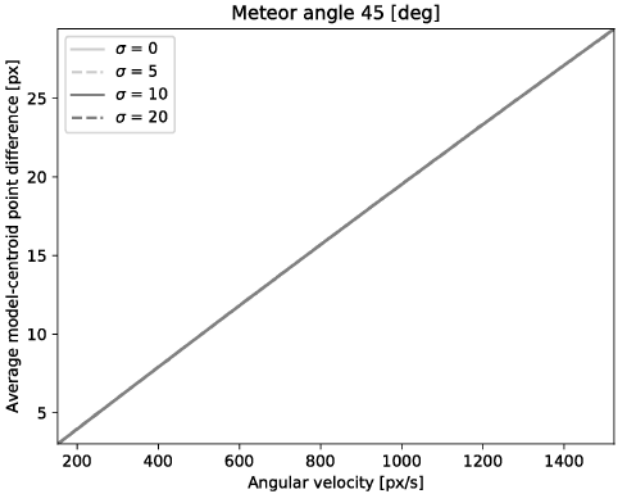

Figure 7 – Centroid offset in relation to the meteor velocity (given in px/s). The centroid offset dominates, thus all noise levels share the same line.

Based on these results, two methods of meteor centroid correction were developed. A temporal correction which corrects the time of a given centroid using minimal information (Section 2.2), and a spatial correction which corrects the image coordinates of the centroid with a uniform time sampling, but requires estimating the meteor angle and instantaneous velocity from the imagery (Section 2.3).

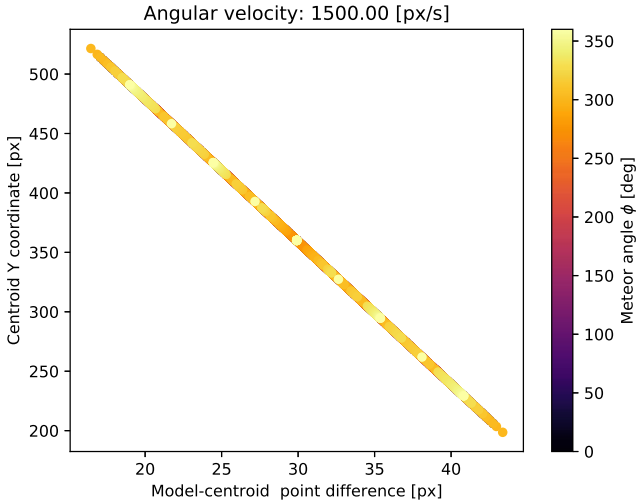

Figure 8 – The velocity is fixed at an extreme value of 1500 px/s, while the Y coordinate of the centroid and the correction distance are plotted. Different meteor angles are shown in different colors, but not all colors are visible because they overlap each other.

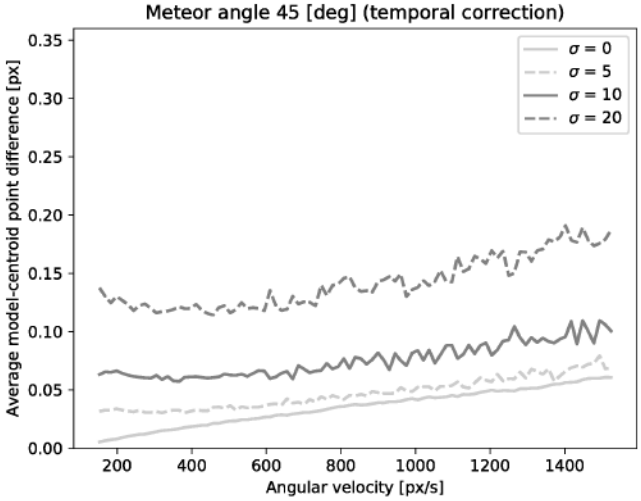

Figure 9 – The centroid offset in relation to the velocity. The temporal correction is applied to the centroid coordinates.

2.2 Temporal correction

Because the centroid offset is highly dependent on the vertical position of the meteor on the image, it is possible to correct for the rolling shutter effect by simply modifying the time stamps of the centroids. This of course will result in a variable time sampling out of sync with the frame time for each centroid position of each meteor image, rather than the uniform time sampling experienced with a global shutter.

First, it should be noted as to the way absolute time is computed from video frames. For global shutters this should be the middle of the exposure period for a given frame. For rolling shutters care must be taken to account for exposure times less than the frame time and when a camera time stamps the image. For now, we will assume that any small bias in absolute time will be corrected for later during trajectory estimation. Thus the relative time of every frame from some reference time can be computed with the following equation:

$$t_{frame} = \frac{i_{frame}}{FPS} \tag{9}$$

where i_{frame} is the index of the frame since the beginning of the meteor, and FPS is the frames per second of the camera.

In rolling shutter cameras, each pixel row starts its exposure at a slightly later time after the row above, and the time delay between each pixel row depends on the number of rows in the image. The time delay between the start of each subsequent row is:

$$\Delta t = \frac{1}{FPS}\frac{1}{n_{rows}} \tag{10}$$

where n_{rows} is the size of the image's Y axis in pixels (i.e. the vertical dimension). Assuming that the rolling shutter starts integrating from the top, the time of every row y_i is then:

$$t_{row} = y_i \Delta t \tag{11}$$

The Y coordinate of the meteor centroid hence determines the time at which the meteor centroid was captured. Including a time bias t_f based on f, the ratio of exposure time to the frame-to-frame time divided by the frame rate FPS, corrects the rolling shutter time into one that is synchronized with a global shutter (assumes the rolling shutter centroids are computed just after the last row is read out). f was defined as:

$$f = t_{exposure} FPS \tag{12}$$

where $t_{exposure}$ is the exposure time.

The rolling shutter centroids will thus fall on the global shutter track at the appropriate time. It only remains for the user to determine the global shutter bias relationship to absolute time. Thus the corrected relative time can be computed as:

$$t'_{frame} = t_{frame} - t_{row} - t_f = \frac{1}{FPS}\left(i_{frame} - \frac{y_i}{n_{rows}} - f\right) \tag{13}$$

where y_i is the Y coordinate of the rolling shutter centroid.

The performance of the temporal correction was tested by applying it to simulated centroids of noisy, decelerating meteors with an angle of $\varphi = 45°$ and a range of velocities. The final meteor velocity was 90% of the initial velocity, and the duration of the meteor was a multiple of the frame time ($1/FPS$). The a parameter used to model meteor deceleration was fixed at the value of 0.06', while the b parameter was computed using methods described in Section 2.1. We computed the difference in pixels from the true (model) and computed centroid positions. The results are shown in Figure 9. The maximum centroid offset for the highest velocity and the highest level of background noise is under 0.2 pixels, which is comparable to the achievable precision. Only for the highest angular velocities does the correction start to slightly deviate from the theoretical precision.

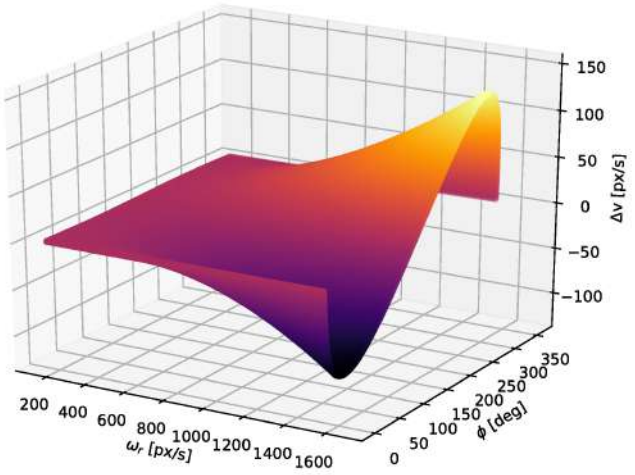

Figure 10 – The dependence of the angular velocity shift on the meteor angle and the observed angular velocity.

2.3 Spatial correction

For certain applications one might want to correct the location of the centroid instead of its time, for example if it is absolutely essential that the points are equally spaced in time as assigned by a frame time. The spatial correction is more complex and involves estimating two parameters of a meteor: the instantaneous angular velocity at every centroid (ω_i) and the meteor angle (φ).

The meteor angle φ was found by fitting a line in the parametric form relating Cartesian to polar coordinates (equation (6), R and φ are fitted) to Y coordinates of centroids versus the distance from the beginning of the meteor – the first centroid at (x_0, y_0) has a distance 0, the final centroid has a distance equivalent to the length of the meteor track.

Next, the instantaneous velocity (ω_i) for each centroid is calculated using the following equation:

$$\omega_i = \frac{\Delta r}{\Delta t} = \frac{r_i - r_{i-1}}{t_i - t_{i-1}} \tag{14}$$

Note that this velocity is given in px/s, rather than '/s. This set of velocities was then smoothed out as instantaneous velocities are sensitive to small measurement errors in centroids. A new value was assigned to each velocity, which was equal to the mean of its two neighbouring velocities:

$$\bar{\omega}_i = \frac{\omega_i + \omega_{i+1}}{2} \tag{15}$$

As the first point does not have a predecessor, we assumed that $\bar{\omega_0} = \bar{\omega_1}$.

Meteors were simulated with velocities ranging from 150 to 1500 px/s, and meteor angles from 0° to 360° using the rolling shutter simulation. We compared the observed angular velocities (computed centroid of the simulated rolling shutter frames) and known angular velocities obtained from equation (2) and found they did not match. In fact, as the rolling shutter effect shifts both the position and the time assigned to each centroid, the angular velocities are also shifted. Computing the difference between the known velocity and the rolling shutter impacted velocity (i.e. the velocity shift), it was found that it is a function of the meteor angle and the observed velocity. The plot of the function is shown in Figure 10. The velocity difference is 0 for a meteor travelling horizontally ($\varphi = 0°$ or $\varphi = 180°$) as the reader meets the meteor in regular intervals. But if the meteor's motion has a vertical component, the reader meets it at different time intervals and the apparent angular velocity changes.

The following equation models this velocity shift, i.e. the value by which the centroid velocity has to be corrected to obtain the true velocity:

$$\Delta\bar{\omega}_i(\bar{\omega}_i, \varphi) = -\bar{\omega}_i \frac{p}{p+1} \tag{16}$$

where p is defined as:

$$p = \sin\varphi \frac{\bar{\omega}_i}{\omega_{ref}} \tag{17}$$

The value of ω_{ref} is defined either as n_{rows} (if the velocity is measured in pixels/frame), as $n_{rows} \times FPS$ (if the velocity is measured in pixels/second) or as $n_{rows} \times FPS \times k$ (if the velocity is measured in arcminutes per second). Here, n_{rows} is the vertical dimension of the image, and FPS is the number of frames per second taken by the camera. Hence the corrected velocity value is:

$$\omega_{corr(i)} = \bar{\omega}_i + \Delta\bar{\omega}_i \tag{18}$$

As it can be seen from Figures 7 and 8, the correction distance is proportional to the meteor's velocity and inversely proportional to its Y coordinate. Additionally, the distance correction was found to be dependent on whether the exposure time is equal to or less than the frame-to-frame time. As it is shown in Figure 11, the value of the f parameter significantly influences the correction distance. Thus a correction formula was constructed which fully accounts for short exposures relative to frame time and the other effects of rolling shutter. The amplitude of the correction distance ΔR_i is dependent on the row value of the bottom most row y_B, the rolling shutter row centroid y_i, the f parameter and the number of rows in the image:

$$\Delta R_i = \frac{\omega_{corr(i)}}{\omega_{ref}} \left(y_B - y_i - (1-f)\, n_{rows}\right) \tag{19}$$

The corrected coordinates of the meteor in Cartesian coordinates are then given by:

$$\begin{aligned} x_{corr} &= x_i + \Delta R_i \cos\varphi \\ y_{corr} &= y_i + \Delta R_i \sin\varphi \end{aligned} \tag{20}$$

It should be noted that the corrections defined herein are independent of where the user defines the origin of the focal plane Cartesian coordinate system. The origin can be the upper left corner, or the center, or some other location in the image. As long as centroid estimates and y_B are defined in the same coordinates.

A test of the performance of the spatial correction was done by applying it to simulated centroids of a decelerating meteor with an angle of $\varphi = 45°$. Computing the residuals in pixels between the true and the

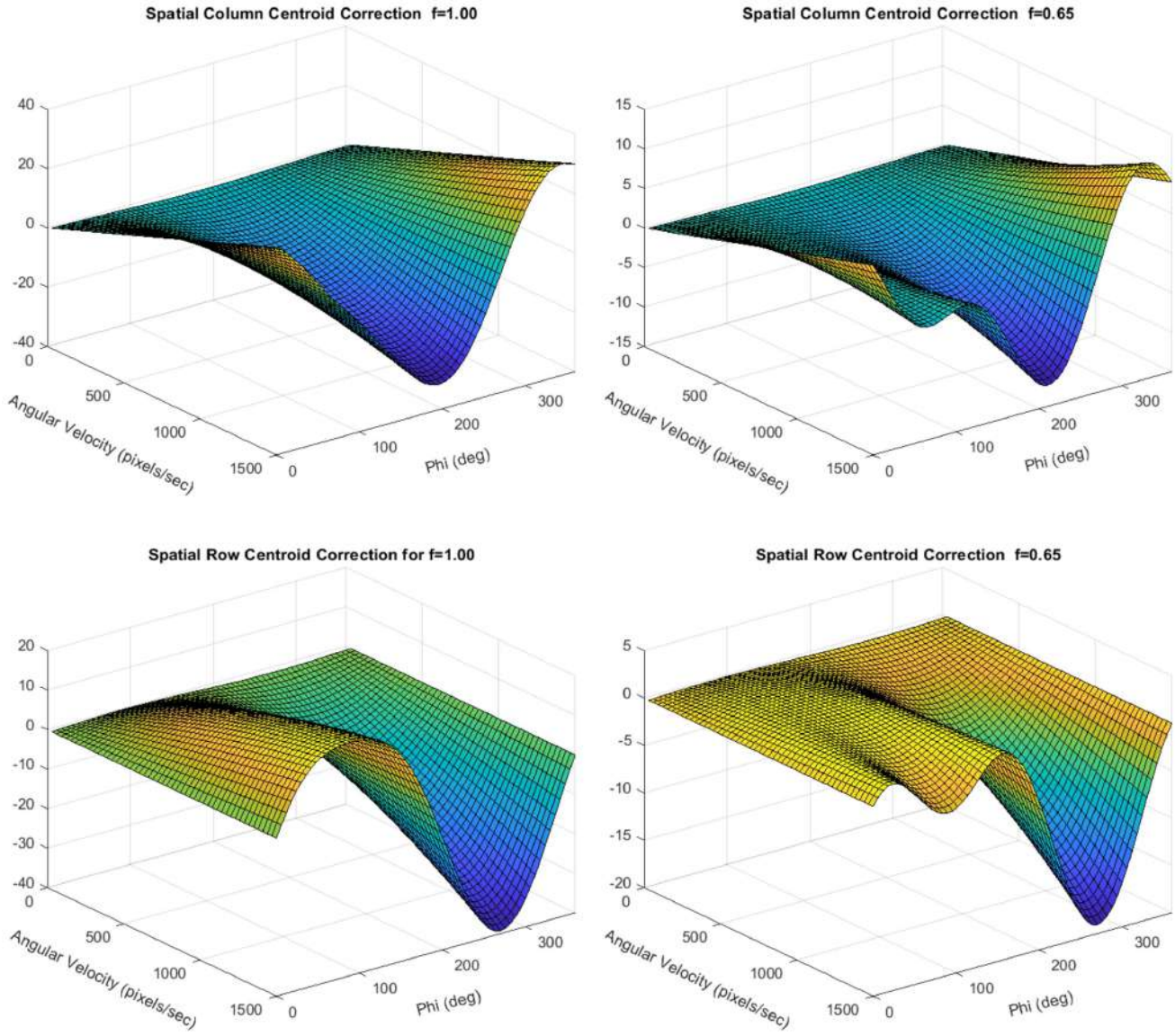

Figure 11 – Different correction distances depending on different values of the f parameter. Shown in relation to angular velocity and meteor angle.

corrected positions, the results are shown in Figure 12. The maximum centroid residual for the highest angular velocity is 0.3 pixels for the largest background noise level, slightly higher than the theoretically achievable precision. The reason for the deviation is the simplicity of the angular velocity smoothing method in a highly decelerating situation – the averaging of neighbouring angular velocities underestimates the true angular velocity due to non-symmetry in velocity before and after the time of interest.

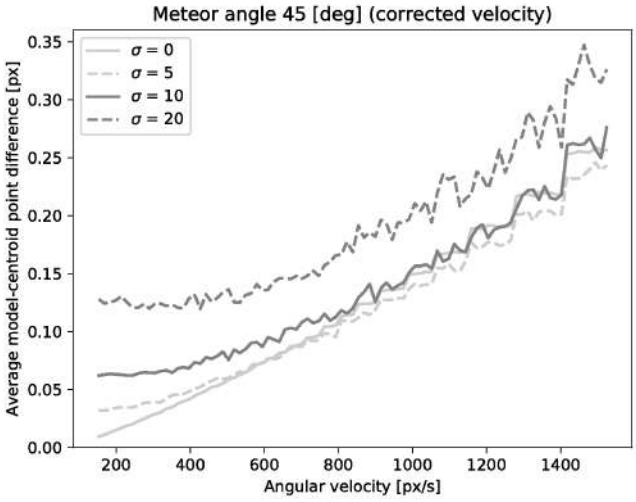

Figure 12 – The centroid offset in relation to the velocity. The spatial correction is applied to centroid coordinates.

2.4 When to apply the rolling shutter corrections

In this section we analyze when does the rolling shutter start to have a significant impact on velocity estimation for a meteor. For this analysis we will assume a worst case scenario of a meteor moving in a vertical direction of the focal plane ($\varphi = 90°$ or $270°$) with the fastest entry velocity of 72 km/s, 90° from the radiant and passing overhead with a range of 70 km.

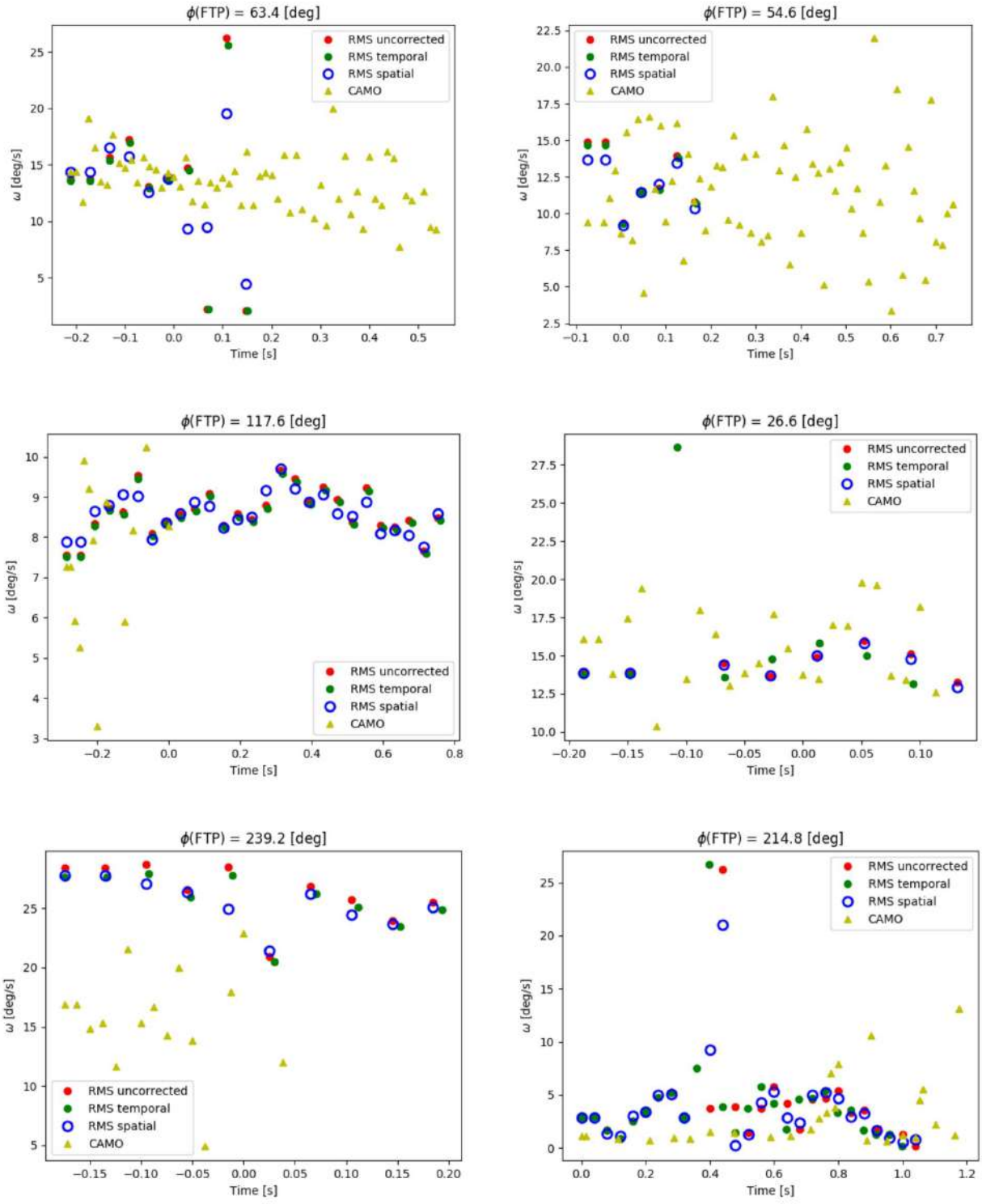

Figure 13 – Comparison of angular velocities obtained from corrected and uncorrected coordinates. 300 '/s corresponds to about 100 px/s. At this speed, the maximum offset in the angular velocity is only 0.2 px/s.

This meteor has the apparent angular velocity ω_{max} of $\sim 60°/\text{s} = 3600'/\text{s}$.

Rearranging the terms in equation (16), and substituting the values mentioned above, we obtain the following expression for a threshold T:

$$T = \frac{\omega_{ref}}{\omega_{max}} = \frac{n_{rows} \times FPS \times k}{3600'/\text{s}} < \frac{100\% - \omega_{err}}{\omega_{err}} \quad (21)$$

where ω_{err} is a given relative velocity error in percent, defined as:

$$\omega_{err} = 100\% \times \frac{\Delta\omega_{max}}{\omega_{max}} \quad (22)$$

When T is less than the right hand side, then the rolling shutter corrections should be employed. For given velocity error tolerances of $\omega_{err} = 5\%$, 2% and 1%, the

right hand side limit is 19, 49 and 99, respectively. Table 1 shows the threshold T computed for various meteor camera systems as if they had rolling shutter sensors.

In general, all-sky systems with rolling shutter cameras do not need to apply corrections except in rare extreme cases with a very tight velocity tolerance of 1%. Moderate and narrow FOV systems do need to apply the corrections. The trend in cameras is to go to larger resolutions and higher frame rates. This helps push the threshold higher, but each designed system should be assessed using the equation above. Also, Sony has announced[a] that low cost global shutter cameras will be out soon, so the need for rolling shutter correction may all be moot in the future. For now, however, this should provide rough guidance as to when to apply the corrections.

3 Results

To verify that the corrected positions and timings of centroids are correct, the correction formulae have been applied to the measurements from an actual rolling shutter camera and compared to a global shutter camera's measurements. A Sony IMX225 rolling shutter camera with a 4 mm lens ($64^\circ \times 35^\circ$ FOV) was installed next to the Canadian Automated Meteor Observatory (CAMO) in Elginfield, Ontario, Canada (Weryk et al., 2013). The CAMO widefield camera is a global shutter camera operated at 80 FPS, with the IMX225 pointed to the same field of view as the CAMO widefield camera. Data from the IMX225 was collected and processed using the RMS meteor detection software (Vida et al., 2016).

To provide evidence of a properly formulated correction, several common meteors between CAMO and the IMX225 had their angular velocities computed. Both the temporal and spatial corrections were applied to measured meteor centroids in the respective image coordinate system for each common meteor. The image coordinates were then transformed to celestial equatorial coordinates using astrometric calibration fits using the RMS library[b].

The spatial and temporal corrections worked as expected by correcting RMS-derived angular velocities closer to CAMO angular velocities. After applying either correction the difference between the corrected and uncorrected angular velocities was rather negligible because moderate field of view cameras observe meteors with relatively low on-chip angular velocities, as was the case with the cameras used. The results are shown in Figure 13.

Utilizing double-station data from two RMS systems running rolling shutter cameras, one at Elginfield and the other at Tavistock (both in Ontario, Canada). The systems were 45 km apart and were observing the same volume of the sky, thus the meteor trajectories could be estimated. Having manually paired the events, the trajectories were computed using the least mean squares (Borovička, 1990) meteor trajectory estimation method. Five common events from the night of 2018 June 14 have been observed and their trajectories estimated. Figure 14 shows four of the meteors that were captured.

For every event, the initial velocity was estimated by fitting a line to the first 25% of time versus distance data. Next, the lag was computed (i.e. the difference between the observed time versus distance and the linear extrapolation using a constant initial velocity). As the rolling shutter effect should have an influence on the observed velocity and therefore the deceleration, we compared the observed lags from both sites. Figures 15 through 19 show the comparison of computed lags (i.e. deceleration profiles): left insets show uncorrected lags, middle insets show lags after the spatial correction, and right insets show lags after the temporal correction. As it can be seen, the lags do not show major differences, indicating that the meteor deceleration is not significantly influenced by the rolling shutter effect from the perspective of a particular observer for the camera specifications utilized.

The estimated geocentric radiants and velocities of the observed meteors are given in Table 2. Due to the small distance between the stations, all meteors have unfavourable geometry with convergence angles of only 10° to 15°, which increased the uncertainty in the estimated radiants. Nevertheless, we notice a significant difference in the geocentric velocity (up to 1 km/s), while radiant estimates seem to be rather stable.

4 Conclusion

Currently, the CCD sensors that have been widely used in meteor cameras, are beginning to be phased out, and meteor astronomers are considering the use of low-cost CMOS alternatives, which typically employ rolling shutters. Simulating the rolling shutter effect of CMOS cameras, it can be shown to have a large influence on meteor position measurements when the meteor has high on-chip apparent angular velocity. This paper provides both a spatial and a temporal method of meteor centroid correction. Both of the correction types account for exposure times that may be less than frame-to-frame times, and have been found to be robust to noise and deceleration.

The temporal correction is the simplest, which corrects only the time of the measurement centroid. It requires knowing only the row coordinate of the centroid and the number of rows in the image. However, using this correction approach will result in meteor centroid measurements being sampled non-uniformly in time. Note that astrometric conversion from focal plane coordinates to equatorial or alt-azimuth coordinates should use the rolling shutter estimated centroids. Only the time of the measurement is corrected.

Alternatively, the spatial correction can be used to correct the position of the rolling shutter centroid on the image, which maintains the uniform time sampling at the frame rate. This requires an estimate of the meteor angle and speed across the focal plane, the row

[a]Sony announcement: `https://www.sony.net/SonyInfo/News/Press/201802/18-018E/index.html`, accessed July 25, 2018

[b]RMS GitHub library: `https://github.com/CroatianMeteorNetwork/RMS`

Table 1 – Comparison of precision thresholds for different camera systems. FOV is the field of view of the vertical image direction.

System	FOV	n_{rows}	FPS	k ['/px]	T
All-sky Full HD	all-sky 180°	1080	25	10	75
RMS 720p, 1*	moderate 35°	720	25	2.9	15
CAMS 720p, 2*	moderate 22°	720	25	1.8	9
CAMS Full HD, 2*	moderate 22°	1080	25	1.2	9
Kowa 55mm f/1.0 720p, 3*	telescopic 4°	720	25	0.5	2.5
50mm ASI120	telescopic 2.5°	960	30	0.16	1.3

1* - (Vida et al., 2018); 2* - (Jenniskens et al., 2011); 3* - (Šegon et al., 2015)

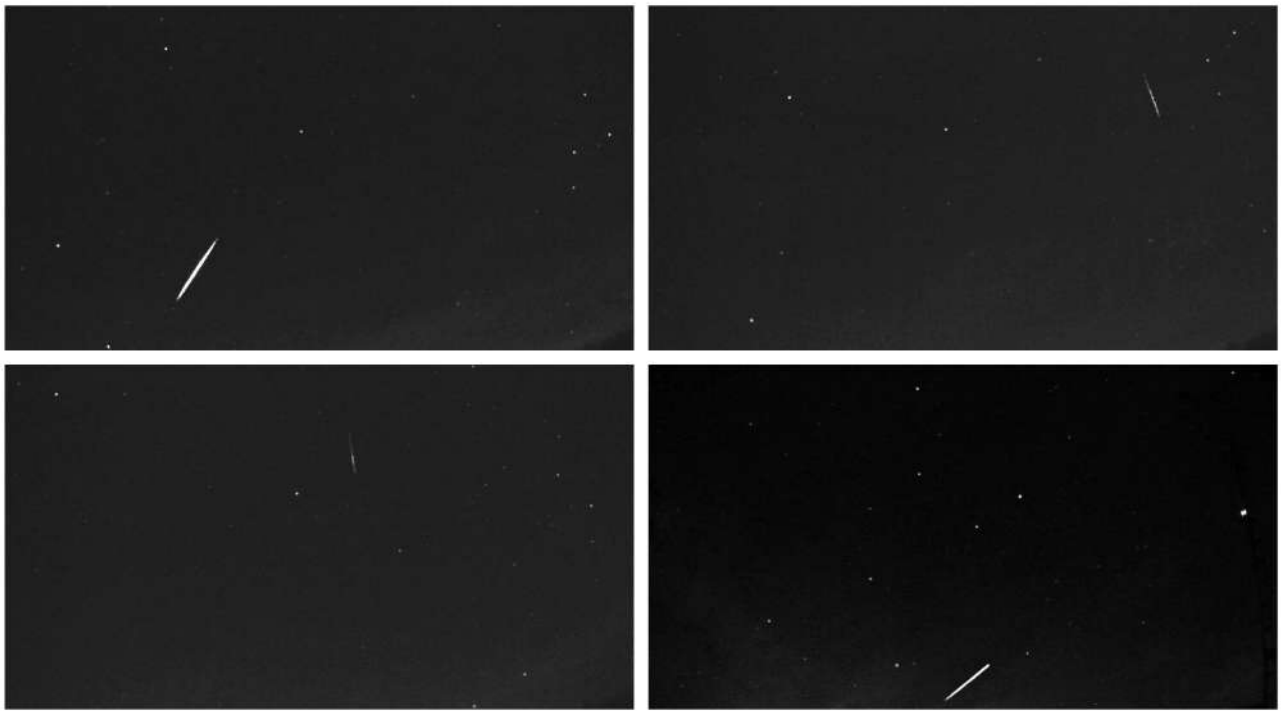

Figure 14 – Four of the meteors imaged with the two RMS systems on 2018 June 14.

of the rolling shutter centroid, the row coordinate of the bottom row in the image, the number of rows in the image, frame rate, exposure to frame time ratio, and pixel angular extent. The "corrected" positions of the rolling shutter centroids are used to generate equatorial or alt-azimuth coordinates via standard astrometry.

To confirm the validity of these corrections we have first tested them on simulated video sequences of meteors in various speeds, orientations, and sensor configurations. Then we compared angular velocities of real observed meteors obtained using a rolling shutter camera and a global shutter camera. We also applied the spatial and temporal corrections on real double station meteor observations collected using rolling shutter cameras. Using the formulations provided herein, correct track positions and apparent angular velocities were obtained. It is apparent that the rolling shutter effect can impact the estimated velocity and should be corrected for using the provided methods.

5 Acknowledgements

We thank Dr. Peter Brown and Dr. Margaret Campbell-Brown for kindly allowing us to use CAMO data.

6 Author Contributions

PK did most of the coding and wrote most of the manuscript, PG developed the temporal correction, improved the spatial correction, added the correction for short exposure times, independently confirmed the Python simulations and performed final edits on the paper, DV provided the initial code, provided guidance and wrote parts of the manuscript, DŠ provided guidance and coordination, and AM tested IP cameras and other hardware used for this work.

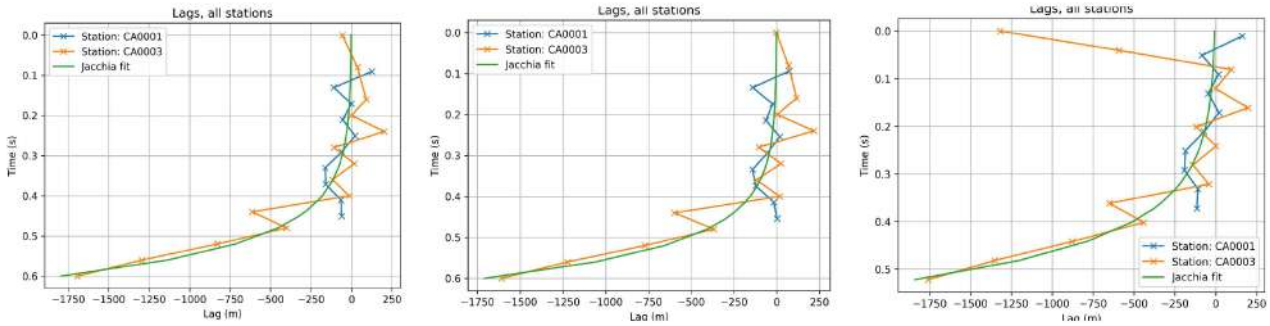

Figure 15 – Meteor of 2018 June 14, $06^{h}07^{m}20^{s}$ UTC; Left: Uncorrected meteor coordinates. Middle: Spatially corrected coordinates. Right: Temporally corrected coordinates.

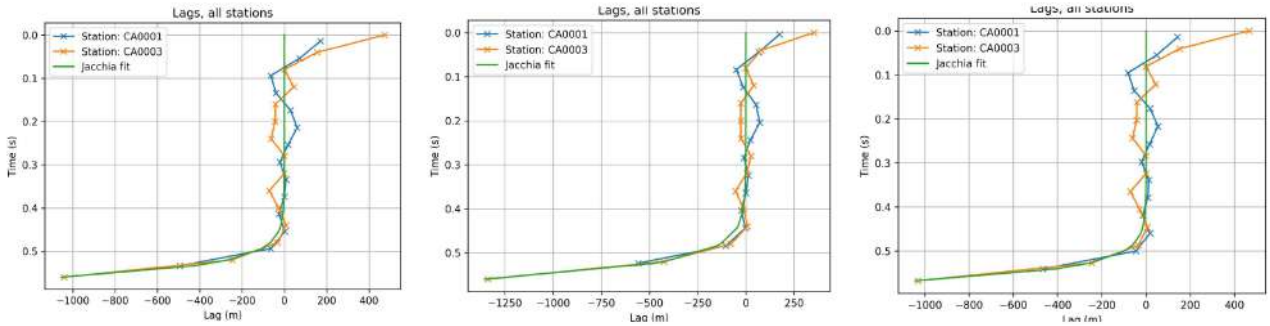

Figure 16 – Meteor of 2018 June 14, $06^{h}26^{m}58^{s}$ UTC; Left: Uncorrected meteor coordinates. Middle: Spatially corrected coordinates. Right: Temporally corrected coordinates.

References

Borovička J. (1990). "The comparison of two methods of determining meteor trajectories from photographs". *Bulletin of the Astronomical Institutes of Czechoslovakia*, **41**, 391–396.

Brown P., Weryk R., Kohut S., Edwards W., and Krzeminski Z. (2010). "Development of an all-sky video meteor network in Southern Ontario, Canada The ASGARD System". *WGN, Journal of the International Meteor Organization*, **38**, 25–30.

Ceplecha Z. (1987). "Geometric, dynamic, orbital and photometric data on meteoroids from photographic fireball networks". *Bulletin of the Astronomical Institutes of Czechoslovakia*, **38**, 222–234.

Jacchia L. G. and Whipple F. L. (1961). "Precision orbits of 413 photographic meteors". *Smithsonian Contributions to Astrophysics*, **4**, 97–129.

Jenniskens P., Gural P., Dynneson L., Grigsby B., Newman K., Borden M., Koop M., and Holman D. (2011). "CAMS: Cameras for Allsky Meteor Surveillance to establish minor meteor showers". *Icarus*, **216:1**, 40–61.

Samuels D., Wray J., Gural P. S., and Jenniskens P. (2014). "Performance of new low-cost 1/3" security cameras for meteor surveillance". In *Proceedings of the 2014 International Meteor Conference, Giron, France*. pages 18–21.

Šegon D., Andreić Ž., Korlević K., and Vida D. (2015). "Croatian Meteor Network: ongoing work 2014–2015". In *Proceedings of the International Meteor Conference, Mistelbach, Austria*. pages 27–30.

Vida D., Mazur M., Segon D., Zubovic D., Kukic P., Parag F., and Macan A. (2018). "First results of a Raspberry Pi based meteor camera system". *WGN, Journal of the International Meteor Organization*, **46:2**, 71–78.

Vida D., Zubović D., Šegon D., Gural P., and Cupec R. (2016). "Open-source meteor detection software for low-cost single-board computers". In *Proceedings of the International Meteor Conference (IMC2016), Egmond, The Netherlands*. pages 2–5.

Weryk R., Campbell-Brown M., Wiegert P., Brown P., Krzeminski Z., and Musci R. (2013). "The Canadian automated meteor observatory (CAMO): system overview". *Icarus*, **225:1**, 614–622.

Handling Editor: Javor Kac
This paper has been typeset from a LaTeX file prepared by the authors.

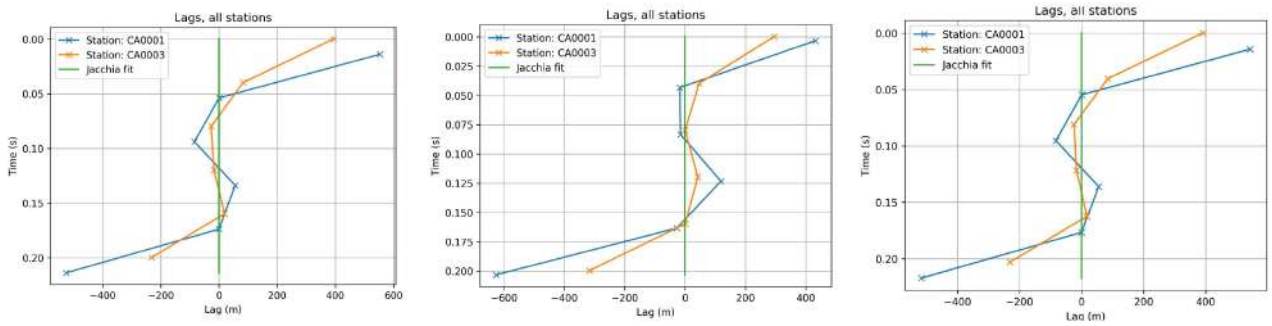

Figure 17 – Meteor of 2018 June 14, $07^{h}28^{m}09^{s}$ UTC; Left: Uncorrected meteor coordinates. Middle: Spatially corrected coordinates. Right: Temporally corrected coordinates.

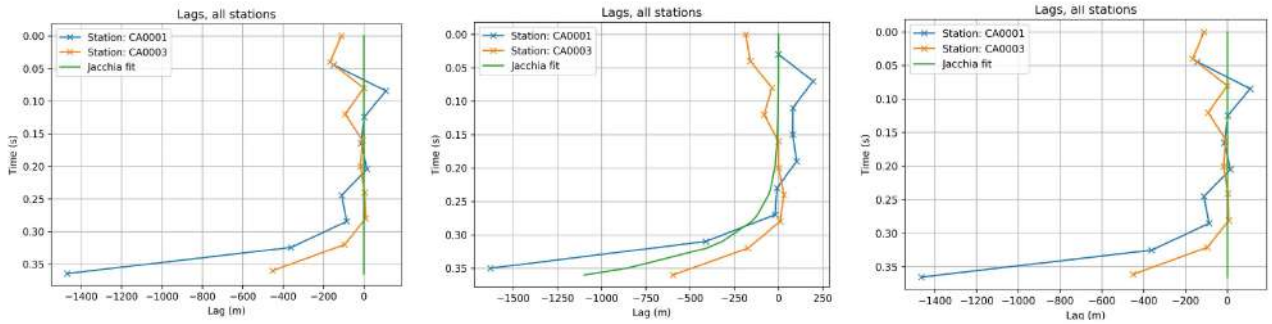

Figure 18 – Meteor of 2018 June 14, $07^{h}46^{m}21^{s}$ UTC; Left: Uncorrected meteor coordinates. Middle: Spatially corrected coordinates. Right: Temporally corrected coordinates.

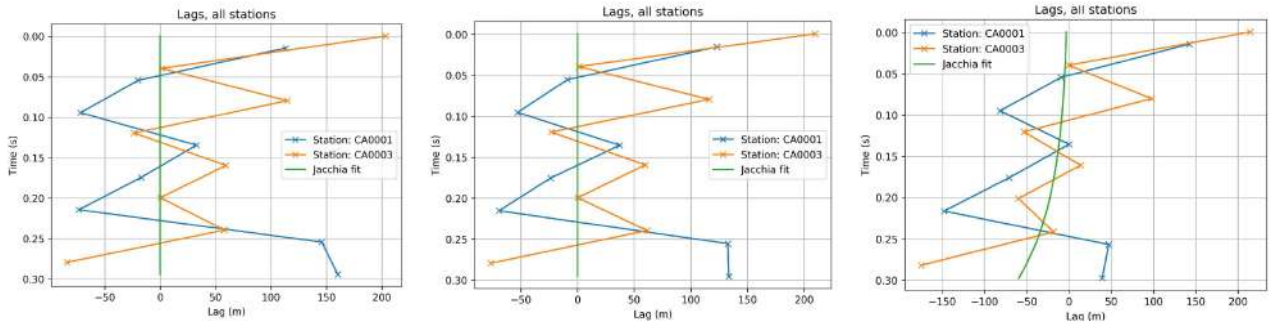

Figure 19 – Meteor of 2018 June 14, $07^{h}52^{m}12^{s}$ UTC; Left: Uncorrected meteor coordinates. Middle: Spatially corrected coordinates. Right: Temporally corrected coordinates.

Table 2 – Comparison of geocentric radiants and velocities for observed meteors. RA and Dec are given in degrees and V_g in km/s. The "Corr" column indicates the type of correction applied: O – original (no correction), S – spatial, T – temporal.

Time	Corr	RA_g	Dec_g	V_g
2018-06-14 $06^{h}07^{m}20^{s}$	O	228.14	+0.66	11.42
	S	228.53	+0.65	11.85
	T	227.61	+2.72	11.75
2018-06-14 $06^{h}26^{m}58^{s}$	O	315.36	+35.90	54.39
	S	315.38	+35.50	53.61
	T	315.37	+35.90	53.56
2018-06-14 $07^{h}28^{m}09^{s}$	O	317.77	+31.49	53.77
	S	317.85	+31.19	52.92
	T	317.77	+31.48	52.80
2018-06-14 $07^{h}46^{m}21^{s}$	O	11.91	+76.83	28.60
	S	13.03	+77.05	28.81
	T	11.91	+76.72	28.36
2018-06-14 $07^{h}52^{m}13^{s}$	O	274.54	−11.34	32.52
	S	274.52	−11.09	32.42
	T	274.31	−10.66	32.57

Preliminary results

Results of the IMO Video Meteor Network — December 2017

Sirko Molau[1], *Stefano Crivello, Rui Goncalves, Carlos Saraiva, Enrico Stomeo, Jörg Strunk, and Javor Kac*

The IMO Video Meteor Network cameras recorded over 46 000 meteors in nearly 9 800 hours of observing time during 2017 December. Flux density and population index profiles are presented for the Geminids and the Ursids. The annual summary of the 2017 IMO Video Meteor Network observations is presented. More than 425 000 meteors were recorded in over 116 000 hours of observing time.

Received 2018 October 21

1 Introduction

With over 46 000 meteors from 9 800 hours effective observing time (Table 4 and Figure 1), the output of December 2017 was below the results of the two preceding years. In particular in northern Europe we had several intervals with poor weather, where we could not observe for several days in a row. Exactly half of the 80 active video cameras managed to observe during twenty or more nights, but even the observers in southern Europe with their often-favorable conditions rarely passed 25 nights.

2 Geminids

Given the poor weather, there was little benefit obtained from the waning moon having hardly interfered with the Geminid peak, because you need both good lunar *and* good weather conditions. Figure 2 presents the flux density profile of this last major shower in 2017 in comparison with the three preceding years. Whereas the activity profile of 2016 was of poor quality and the

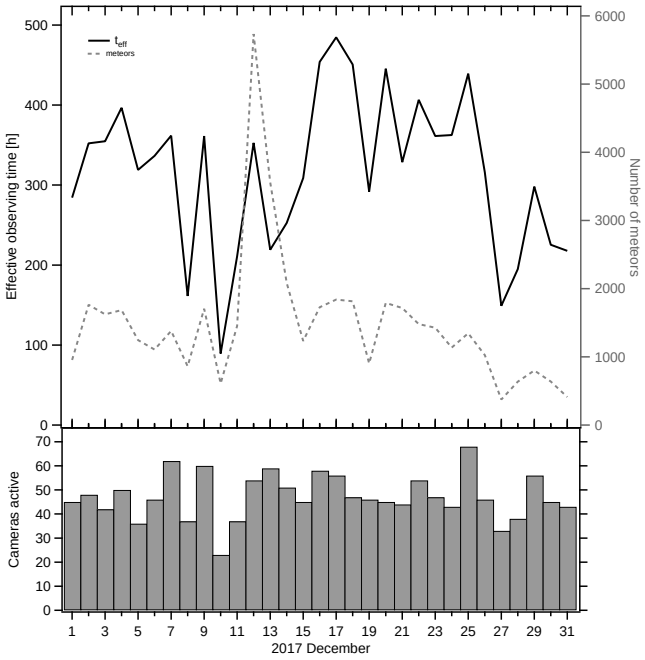

Figure 1 – Monthly summary for the effective observing time (solid black line), number of meteors (dashed gray line) and number of cameras active (bars) in 2017 December.

[1]Abenstalstr. 13b, 84072 Seysdorf, Germany.
Email: sirko@molau.de

IMO bibcode WGN-465-molau-viddec
NASA-ADS bibcode 2018JIMO...46..166M

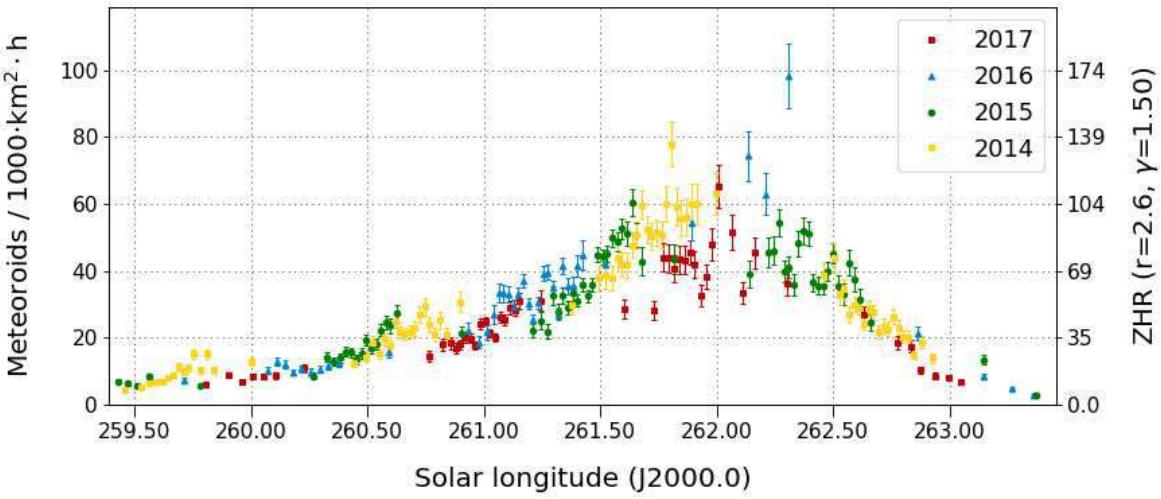

Figure 2 – Comparison of the flux density profile of the Geminids in 2014–2017, derived from video data of the IMO Network.

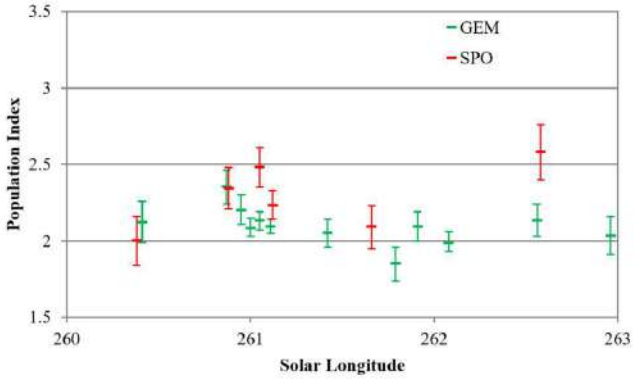

Figure 3 – Population index of the Geminids (lighter/green) and sporadic meteors (darker/red) in December 2017.

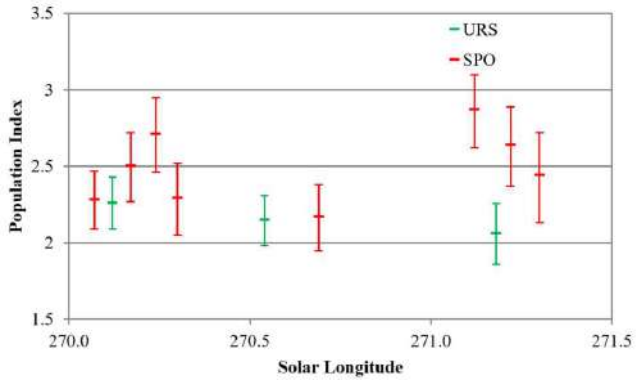

Figure 5 – Population index of the Ursids (lighter/green) and sporadic meteors (darker/red) in December 2017.

flux density was strongly overestimated (in fact, after another analysis we deleted some data sets from December 2016 that had a zero effective collection area, yet still recorded many Geminids through cloud gaps), the activity values in 2017 were below the average. Once more there is quite some scatter in the data, because right in the maximum night the weather conditions were fairly poor.

With $r = 2.1$, the population index of the Geminids (Figure 3) was only marginally smaller than the sporadic population index ($r = 2.3$). The profile is rather flat – fluctuations are probably caused by the insufficient data set.

3 Ursids

The observing conditions were somewhat better during the Ursids, but in northern Europe also this shower disappeared behind clouds. Whereas we had recorded occasional outbursts earlier this decade, the Ursids remained inconspicuous in 2017 just as in the two preceding years. The activity of 2015 to 2017 (Figure 4) shows a similar profile with significant activity between 270° and 271.°5 solar longitude, and a peak flux density of about 10 meteoroids per 1 000 km^2 per hour between 270.°5 and 271° solar longitude (December 22). The time of peak activity varies a bit, but the shape of the profile remains the same.

With $r = 2.2$, the population index of the Ursids is similarly as "unspectacular" as that of the Geminids (Figure 5).

4 New database

At this point we would like to mention a new meteor database. In spring 2018, Jure Zakrajšek started to import the meta data of his observations into an Access database. After some discussion with Sirko Molau the idea was born, to store the meta data of the whole IMO Network, which are currently maintained manually in a big Excel spreadsheet, in that database. Not only is a database less error-prone, but it is also more flexible and allows for additional analyses with only little effort, for example.

In the months that followed, Jure and Sirko invested some considerable time to import the meta data of all MetRec logfiles since 1993 into the database. We stumbled across a number of minor inconsistencies, which were localized and fixed to maintain the high quality of the IMO Video Meteor Database. In the end there was zero deviation between the Excel spreadsheet and the database. In fact, the new database is even more

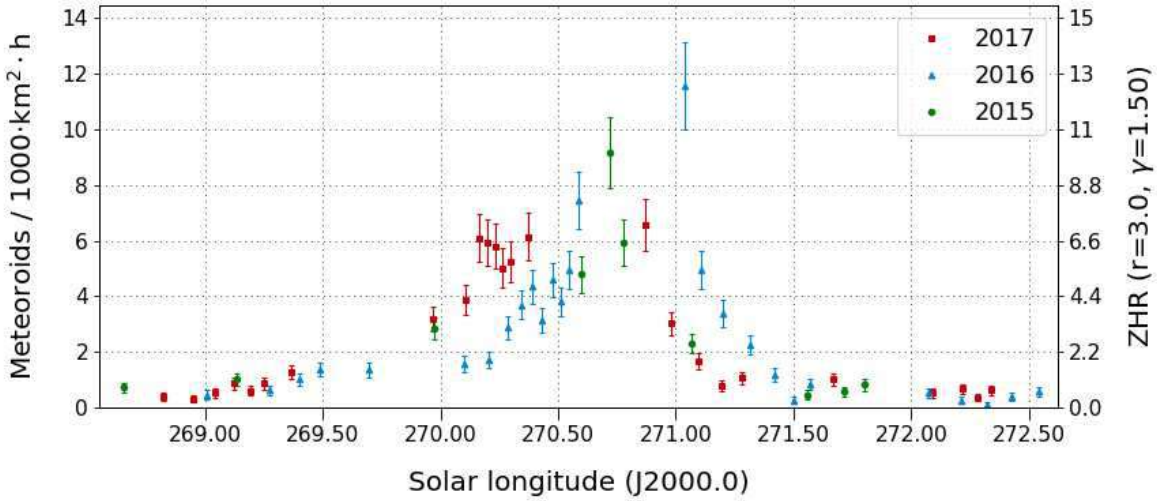

Figure 4 – Comparison of the flux density profile of the Ursids in 2015–2017, derived from video data of the IMO Network.

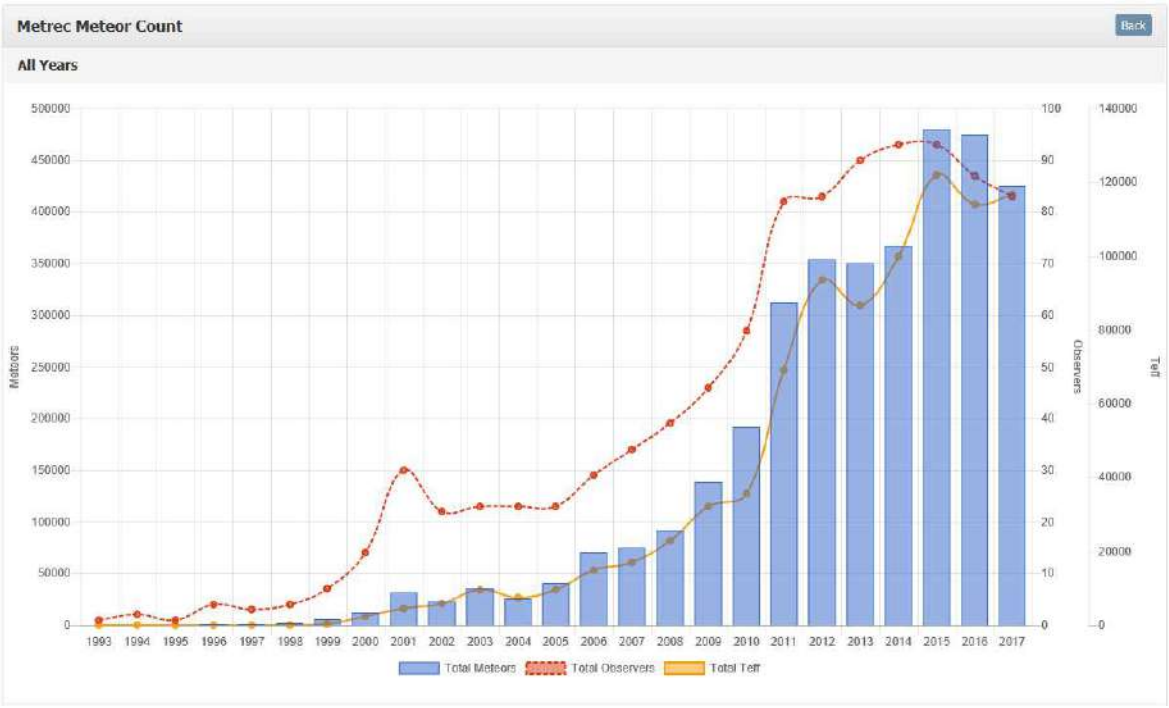

Figure 6 – Comparison of the number of observers, meteors, and the effective collection area in the IMO Video Meteor Database between 1993 and 2017.

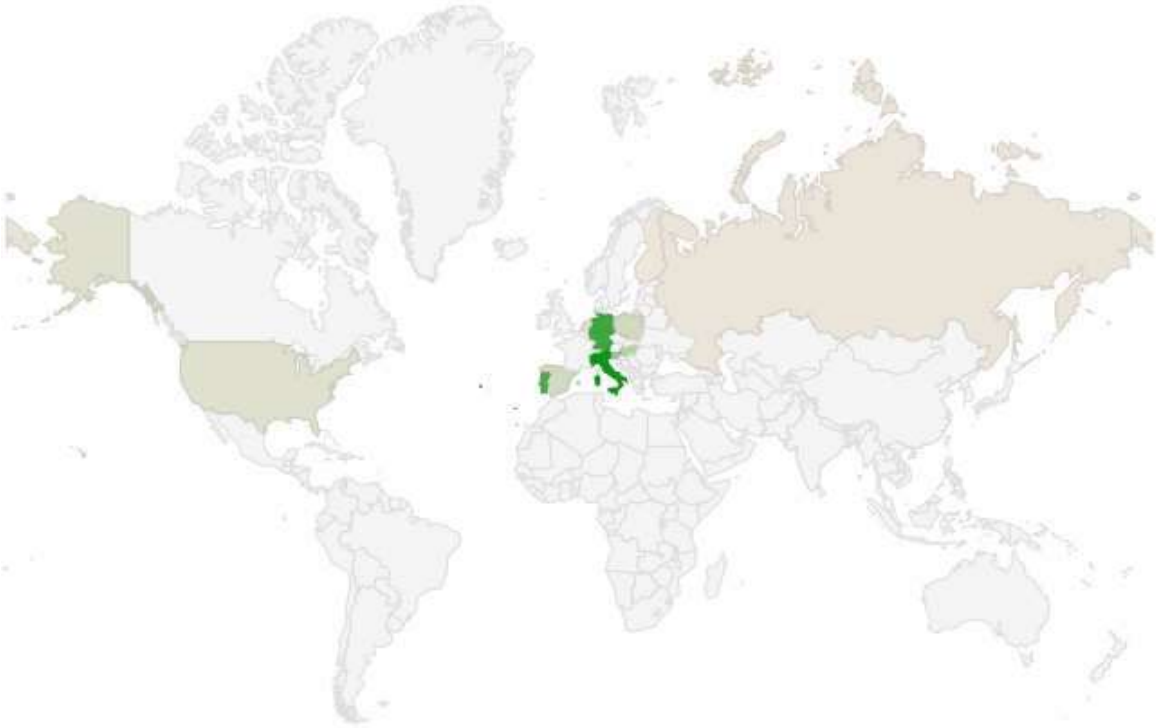

Figure 7 – Country distribution of meteors recorded in 2017.

comprehensive than previous sources, because missing information was extracted and manually added from other sources such as the monthly reports.

The following annual report already contains a few figures created from the new database. Before we publish it via the Internet, we first need to run some final consistency checks, migrate the database to PostgreSQL and relocate the user interface to the IMO network webserver. Once that is completed, we will publish the URL.

5 2017 summary of the IMO Video Network

In 2017 we saw another small decrease in the number of active video cameras. In the 19th year of the IMO Network, 41 observers (2016: 44) from 11 countries

Table 1 – Monthly distribution of video observations in the IMO Network 2017.

Month	Observing Nights	Eff. Observing Time	Meteors	Meteors / Hour
January	31	11 947.3	33 601	2.8
February	28	7 119.5	14 593	2.0
March	31	10 534.8	19 938	1.9
April	30	8 267.7	16 252	2.0
May	31	7 319.1	16 187	2.2
June	30	7 252.9	18 741	2.6
July	31	8 457.3	35 690	4.2
August	31	12 751.6	78 489	6.2
September	30	9 926.4	35 898	3.6
October	31	13 123.2	67 253	5.1
November	30	10 107.8	42 628	4.2
December	31	9 787.1	46 067	4.7
Overall	365	116 594.7	425 337	3.6

(2016: 12) participated with overall 82 meteor cameras (2016: 85) in the IMO Network. Top scorer with respect to the number of cameras was Germany (19), followed by Italy and Portugal (13 each). Ten cameras were operated in Slovenia and Hungary, six in Poland, four in Spain, two in the US and one in the Netherlands, Finland and Russia.

Figure 6 shows that the decrease in meteor cameras had no impact on the effective observing time, which was just in-between the results of 2015 and 2016. However, the number of recorded meteors reduced by 10%, which mainly reflects the long breakdown of the CILBO cameras on the Canary Islands.

In 365 observing nights (2016: 366) and 116 595 observing hours (2016: 113 937) we recorded a total of 425 337 meteors (2016: 474 658). The average count went down to 3.6 meteors per hour and reached the lowest value in the last 15 years.

Figure 7 depicts how many meteors were recorded in each country in 2017. It is obvious that most observations still originate from southern and central Europe. A closer look reveals that Italy is plotted marginally darker than Germany. In fact, even though there were less cameras operated in 2017, the effective observing time of Italian cameras was by 8% larger than that of the German cameras, and the meteor count was even larger by 25%. The competitive edge of the German observers with respect to the meteor count has shrunk to 2% in the overall statistics, and we expect that the Italian observers will take over the lead in 2018.

Table 1 shows the monthly distribution of video meteor observations. The average output was slightly below 10 000 hours per month, but October and August 2017 ranked 3rd and 4th in the long-term statistics of the IMO Network. In January and October 2017, we recorded more meteors than ever before in these months.

Nine observers (one more than in 2016) managed to collect data during more than 300 observing nights. On top we find the "usual suspects", whereby in 2017 the Portuguese observers Rui Goncalves (348 nights) and Rui Marques (341 nights) outpaced Sirko Molau (339 nights). Further observers from Italy, Portugal and the US follow a short distance behind.

With respect to the effective observing time, we had two observers in 2017 (Rui Goncalves and Carlos Saraiva) who collected more than 10 000 hours. With respect to the meteor count, however, Sirko Molau was again the top scorer. Overall 12 observers (one more than in 2016) provided over 10 000 meteors to the video database.

Table 3 presents the details for all active observers in the IMO Network in 2017. The number of cameras and stations refers to the major part of the year.

Table 2 – The ten most successful video systems in 2017.

Camera	Location	Observer	Observing Nights	Eff. Observing Time [h]	Meteors	Meteors / h
Salsa3	Tucson (US)	Carl Hergenrother	326	2 707.6	6 593	2.4
Cab1	Lisbon (PT)	Rui Marques	326	2 612.8	9 234	3.5
Templar1	Tomar (PT)	Rui Goncalves	325	2 544.3	10 463	4.1
Templar2	Tomar (PT)	Rui Goncalves	320	2 525.6	8 541	3.3
Templar4	Tomar (PT)	Rui Goncalves	319	2 409.5	8 843	3.7
Mario	Faenza (IT)	Mario Bombardini	319	2 131.3	10 883	5.1
Sco38	Scorze (IT)	Enrico Stomeo	318	1 867.5	11 193	6.0
Templar5	Tomar (PT)	Rui Goncalves	317	2 213.1	7 896	3.6
Bilbo	Valbrevenna (IT)	Stefano Crivello	316	2 087.0	10 180	4.9
Noa38	Scorze (IT)	Enrico Stomeo	315	1 848.5	9 877	5.3

Table 3 – Distribution of video observations over the observers in 2017.

Observer	Country	Observing Nights	Eff. Observing Time [h]	Meteors	Meteors / h	Cameras (Stations)
Rui Goncalves	Portugal	348	13 073.2	40 966	3.1	6 (1)
Rui Marques	Portugal	341	4 725.3	16 111	3.4	2 (1)
Sirko Molau	Germany	339	9 851.3	49 563	5.0	7 (2)
Stefano Crivello	Italy	338	6 916.9	34 880	5.0	4 (1)
Carlos Saraiva	Portugal	336	10 643.7	26 049	2.4	5 (1)
Enrico Stomeo	Italy	334	5 488.4	32 248	5.9	3 (1)
Carl Hergenrother	USA	326	2 707.6	6 593	2.4	1 (1)
Mario Bombardini	Italy	319	2 131.3	10 833	5.1	1 (1)
Francesca Cineglosso	Italy	307	1 777.4	7 851	4.4	1 (1)
István Tepliczky	Hungary	294	3 031.7	7 924	2.6	2 (2)
Mitja Govedič	Slovenia	292	2 793.8	7 243	2.6	1 (1)
Javor Kac	Slovenia	286	6 132.2	28 049	4.6	5 (3)
Jörg Strunk	Germany	281	5 081.9	16 542	3.3	5 (1)
Zsolt Perkó	Hungary	280	1 682.7	6 929	4.1	1 (1)
Antal Igaz	Hungary	279	2 258.0	3 198	1.4	2 (2)
Rainer Arlt	Germany	276	1 224.9	6 658	5.4	1 (1)
Bernd Klemt	Germany	272	2 443.8	7 149	2.9	2 (2)
Károly Jónás	Hungary	271	2 953.2	5 844	2.0	1 (1)
Flavio Castellani	Italy	265	2 075.0	6 602	3.2	1 (1)
József Morvai	Hungary	265	1 511.4	2 985	2.0	1 (1)
Maurizio Carli	Italy	263	1 831.3	12 274	6.7	1 (1)
Hans Schremmer	Germany	261	1 349.7	3 738	2.8	1 (1)
Mike Otte	USA	251	1 327.3	2 579	1.9	1 (1)
Maciej Maciejewski	Poland	250	4 115.4	14 280	3.5	4 (1)
Maurizio Eltri	Italy	240	1 492.0	5 851	3.9	1 (1)
Martin Breukers	Netherlands	234	1 119.2	2 744	2.5	1 (1)
Wala Węgrzyk	Poland	231	973.2	2 622	2.7	1 (1)
Leo Scarpa	Italy	230	1 329.3	2 212	1.7	1 (1)
Stane Slavec	Slovenia	228	2 142.9	4 938	2.3	2 (1)
Wolfgang Hinz	Germany	227	1 202.4	4 075	3.4	1 (1)
Fabio Moschini	Italy	202	1 073.3	3 572	3.3	1 (1)
Eckehard Rothenberg	Germany	194	1 001.2	2 411	2.4	1 (1)
Kevin Förster	Germany	182	990.8	4 090	4.1	1 (1)
Alvaro Lopes	Portugal	172	1 155.8	1 804	1.6	1 (1)
Detlef Koschny	Netherlands	158	2 732.5	17 962	6.6	4 (2)
Mikhail Maslov	Russia	152	630.1	2 841	4.5	1 (1)
Paolo Ochner	Italy	151	976.4	2 842	2.9	1 (1)
Erno Berkó	Hungary	130	918.8	5 428	5.9	1 (1)
Ilkka Yrjölä	Finland	120	618.5	1 525	2.5	1 (1)
Jure Zakrajšek	Slovenia	96	589.2	1 457	2.5	1 (1)
Tomasz Łojek	Poland	90	506.5	1 841	3.6	1 (1)
Péter Bánfalvi	Hungary	8	15.3	34	2.2	1 (1)

In the list of the Top-10 video cameras (Table 2), the bar was up again significantly. Whereas barely 300 observing nights were sufficient in 2016, it had to be 315 nights in 2017. Indeed, there were five cameras with over 300 observing nights that did not made it into the Top-10.

The following cameras, which recorded more than 10 000 meteors, are also absent from the list: Stg38 (13 640), Bmh2 (12 274), Avis2 (11 347) and Min38 (11 178).

The complete dataset from 1993 to 2017 is now available for download at the IMO Network homepage `http://www.imonet.org`. With 2017 included, the database has grown to 3 514 296 meteors from 864 879 hours effective observing time during 6 469 nights.

As always, we would like to thank to the committed video observers who contributed to the IMO Network. Particular thanks to Stefano Crivello, Enrico Stomeo, Rui Goncalves, Carlos Saraiva, Maciej Maciejewski and Jörg Strunk, who check every month together with Sirko Molau the consistency of the data set and ensure the high quality of the database.

Handling Editor: Javor Kac

Table 4 – Observers contributing to 2017 December data of the IMO Video Meteor Network. Eff.CA designates the effective collection area; the overall number of nights is the number of nights with at least one camera operating, the overall observing time and number of meteors are sums over all cameras.

Code	Name	Location	Camera	FOV [°²]	Stellar LM [mag]	Eff.CA [km²]	Nights	Time [h]	Meteors
ARLRA	Arlt	Ludwigsfelde/DE	Ludwig2 (0.8/8)	1475	6.2	3779	23	89.9	530
BERER	Berkó	Ludányhalászi/HU	Hulud1 (0.8/3.8)	5542	4.8	3847	4	22.8	308
BOMMA	Bombardini	Faenza/IT	Mario (1.2/4.0)	5794	3.3	739	25	201.6	1311
BREMA	Breukers	Hengelo/NL	Mbb3 (0.75/6)	2399	4.2	699	10	35.0	167
BRIBE	Klemt	Herne/DE	Hermine (0.8/6)	2374	4.2	678	14	41.4	249
		Bergisch Gladbach/DE	Klemoi (0.8/6)	2286	4.6	1080	13	44.6	306
CARMA	Carli	Monte Baldo/IT	Bmh2 (1.5/4.5)*	4243	3.0	371	19	195.1	1385
CASFL	Castellani	Monte Baldo/IT	Bmh1 (0.8/6)	2350	5.0	1611	18	190.5	587
CINFR	Cineglosso	Faenza/IT	Jenni (1.2/4)	5886	3.9	1222	24	85.2	816
CRIST	Crivello	Valbrevenna/IT	Arci (0.8/3.8)	5566	4.6	2575	25	165.6	684
			Bilbo (0.8/3.8)	5458	4.2	1772	25	188.6	1137
			C3P8 (0.8/3.8)	5455	4.2	1586	20	156.7	710
			Stg38 (0.8/3.8)	5614	4.4	2007	23	148.3	1029
ELTMA	Eltri	Venezia/IT	Met38 (0.8/3.8)	5631	4.3	2151	15	119.8	640
FORKE	Förster	Carlsfeld/DE	Akm3 (0.75/6)	2375	5.1	2154	9	37.5	167
GONRU	Goncalves	Foz do Arelho/PT	Farelho1 (0.75/4.5)	2286	3.0	208	11	86.5	106
		Tomar/PT	Templar1 (0.8/6)	2179	5.3	1842	22	218.6	1163
			Templar2 (0.8/6)	2080	5.0	1508	21	229.7	1092
			Templar3 (0.8/8)	1438	4.3	571	22	221.3	524
			Templar4 (0.8/3.8)	4475	3.0	442	21	223.9	1064
			Templar5 (0.75/6)	2312	5.0	2259	25	204.7	967
GOVMI	Govedič	Središče ob Dravi/SI	Orion2 (0.8/8)	1447	5.5	1841	22	162.3	605
			Orion4 (0.95/5)	2662	4.3	1043	26	164.4	443
HERCA	Hergenrother	Tucson/US	Salsa3 (0.8/3.8)	2336	4.1	544	26	233.8	967
HINWO	Hinz	Schwarzenberg/DE	Hinwo1 (0.75/6)	2291	5.1	1819	18	71.1	401
IGAAN	Igaz	Hódmezővásárhely/HU	Huhod (0.8/3.8)	5502	3.4	764	22	84.5	239
			Hupol (1.2/4)	3790	3.3	475	13	78.4	113
JONKA	Jonas	Budapest/HU	Husor (0.95/4)	2286	3.9	445	21	135.6	304
			Husor2 (0.95/3.5)	2465	3.9	715	19	134.4	285
KACJA	Kac	Kamnik/SI	Cvetka (0.8/3.8)*	4914	4.3	1842	6	27.0	69
			Rezika (0.8/6)	2270	4.4	840	9	57.8	440
			Stefka (0.8/3.8)	5471	2.8	379	8	24.2	44
		Kostanjevec/SI	Metka (0.8/12)*	715	6.4	640	11	79.5	295
KOSDE	Koschny	Izana Obs./ES	Icc7 (0.85/25)*	714	5.9	1464	25	198.6	1062
			Lic1 (2.8/50)*	2255	6.2	5670	24	245.3	1390
		La Palma/ES	Icc9 (0.85/25)*	683	6.7	2951	13	76.4	951
			Lic2 (3.2/50)*	2199	6.5	7512	15	125.4	1501
LOJTO	Łojek	Grabniak/PL	Pav57 (1.0/5)	1631	3.5	269	8	41.3	223
MACMA	Maciejewski	Chełm/PL	Pav35 (0.8/3.8)	5495	4.0	1584	14	39.8	207
			Pav36 (0.8/3.8)*	5668	4.0	1573	14	76.7	366
			Pav43 (0.75/4.5)*	3132	3.1	319	13	34.3	151
			Pav60 (0.75/4.5)	2250	3.1	281	15	81.7	316

Table 4 – Observers contributing to 2017 December data of the IMO Video Meteor Network – continued from previous page.

Code	Name	Location	Camera	FOV [°²]	Stellar LM [mag]	Eff.CA [km²]	Nights	Time [h]	Meteors
MARRU	Marques	Lisbon/PT	CAB1 (0.75/6)	2362	4.8	1517	25	222.5	1373
			RAN1 (1.4/4.5)	4405	4.0	1241	26	219.8	1224
MASMI	Maslov	Novosibirsk/RU	NOWATEC (0.8/3.8)	5574	3.6	773	11	42.7	346
MOLSI	Molau	Seysdorf/DE	AVIS2 (1.4/50)*	1230	6.9	6152	19	90.4	769
			ESCIMO2 (0.85/25)	155	8.1	3415	15	85.7	169
			MINCAM1 (0.8/8)	1477	4.9	1084	17	79.3	537
		Ketzür/DE	REMO1 (0.8/8)	1467	6.5	5491	23	90.1	460
			REMO2 (0.8/8)	1478	6.4	4778	22	101.5	711
			REMO3 (0.8/8)	1420	5.6	1967	24	123.6	516
			REMO4 (0.8/8)	1478	6.5	5358	22	113.3	670
MORJO	Morvai	Fülöpszállás/HU	HUFUL (1.4/5)	2522	3.5	532	19	104.0	234
MOSFA	Moschini	Rovereto/IT	ROVER (1.4/4.5)	3896	4.2	1292	26	249.8	729
OCHPA	Ochner	Albiano/IT	ALBIANO (1.2/4.5)	2944	3.5	358	20	178.2	556
OTTMI	Otte	Pearl City/US	ORIE1 (1.4/5.7)	3837	3.8	460	22	157.1	353
PERZS	Perkó	Becsehely/HU	HUBEC (0.8/3.8)*	5498	2.9	460	19	144.7	742
ROTEC	Rothenberg	Berlin/DE	ARMEFA (0.8/6)	2366	4.5	911	12	49.3	155
SARAN	Saraiva	Carnaxide/PT	RO1 (0.75/6)	2362	3.7	381	22	207.3	590
			RO2 (0.75/6)	2381	3.8	459	23	224.5	916
			RO3 (0.8/12)	710	5.2	619	25	185.8	890
			RO4 (1.0/8)	1582	4.2	549	26	224.8	383
			SOFIA (0.8/12)	738	5.3	907	24	196.8	702
SCALE	Scarpa	Alberoni/IT	LEO (1.2/4.5)*	4152	4.5	2052	25	182.8	342
SCHHA	Schremmer	Niederkrüchten/DE	DORAEMON (0.8/3.8)	4900	3.0	409	17	64.2	364
SLAST	Slavec	Ljubljana/SI	KAYAK1 (1.8/28)	563	6.2	1294	11	49.6	125
			KAYAK2 (0.8/12)	741	5.5	920	11	60.8	89
STOEN	Stomeo	Scorze/IT	MIN38 (0.8/3.8)	5566	4.8	3270	26	197.4	1534
			NOA38 (0.8/3.8)	5609	4.2	1911	27	208.3	1376
			SCO38 (0.8/3.8)	5598	4.8	3306	28	206.0	1395
STRJO	Strunk	Herford/DE	MINCAM2 (0.8/6)	2354	5.4	2751	14	34.6	377
			MINCAM3 (0.8/6)	2338	5.5	3590	14	29.9	194
			MINCAM4 (0.8/6)	2306	5.0	1412	9	21.7	77
			MINCAM5 (0.8/6)	2349	5.0	1896	11	27.4	119
			MINCAM6 (0.8/6)	2395	5.1	2178	13	29.3	217
TEPIS	Tepliczky	Agostyán/HU	HUAGO (0.75/4.5)	2427	4.4	1036	22	153.6	579
			HUMOB (0.8/6)	2388	4.8	1607	20	122.1	367
WEGWA	Wegrzyk	Nieznaszyn/PL	PAV78 (0.8/6)	2286	4.0	778	21	97.1	337
YRJIL	Yrjölä	Kuusankoski/FI	FINEXCAM (0.8/6)	2337	5.5	3574	3	1.5	5
ZAKJU	Zakrajšek	Petkovec/SI	TACKA (0.8/12)	714	5.3	783	19	129.8	231
* active field of view smaller than video frame						Overall	31	9 787.1	46 067

October Camelopardalid outburst 2018 October 6

Jürgen Rendtel[1], *Sirko Molau*[2]

The October Camelopardalids (281 OCT) which previously had been observed by video only showed a weak but significant maximum on 2018 October 6 near 00^h30^m UT. Visual ZHR, video meteor flux density and radio forward scatter data provide independent confirmation. The current observations indicate that the 2019 return may occur near the calculated position or slightly before.

Received 2018 October 19

1 Introduction

The minor October Camelopardalids (281 OCT) showed short-lived video outbursts first in 2005 and 2006 on October 5/6 (near $\lambda_\odot = 193°$). In the recent years the shower has been detected annually (Molau et al., 2017) and produced a peak at $\lambda_\odot = 192\overset{\circ}{.}58$ repeatedly with an estimated ZHR of about 5. Enhanced activity was found last on 2016 October 5 at the predicted position at 14^h45^m UT in radio forward scatter data and video camera data from Finland.

The IMO Shower Calendar for 2018 (Rendtel, 2017) describes that assuming a long-period parent, and using the 2005 outburst as reference point, Esko Lyytinen mentions that we might see activity near $\lambda_\odot = 192\overset{\circ}{.}529$ in 2018 and 2019. The timing of the possible 2018 event was perfect for European longitudes: the calculated peak time was 2018 October 6, 02^h17^m UT and was shortly before New Moon.

The radiant at $\alpha = 164°$, $\delta = 79°$ is circumpolar for mid-northern and northern latitudes. The lowest position is reached around 23^h local time. For example, the minimum elevation in Berlin is approximately 40°. Seen the fortunate weather in Germany for the expected maximum, we alerted many visual observers. It was clear, that the number of shower meteors potentially was low. Previous analyses of Sugimoto (based on radio forward scatter data) yielded a peak ZHR of about 20–40. In many cases these ZHR seem to be overestimated (Rendtel et al., 2017). If we optimistically assume a ZHR of 20 and a duration of about half an hour (for simplicity just switched on/off), an observer may see 10 shower meteors divided by $\sin h_R$ if the limiting magnitude is +6.5 (h_R is the radiant elevation). The theoretical peak time is shortly after 3^h local time, so that the radiant has reached at least 45° elevation. So the expected number of OCT meteors would be of the order of 5–7; less if the conditions are not as good as assumed.

2 Observations 2018

The map from the IMO web pages shows that seven observers were out, well distributed over Germany, all observing from dark locations and under good conditions (Table 1). There were others observing during this night as well, but not checking for OCT meteors. The number of OCT was not large enough to attract their attention. This underlines that a reminder in case of possible minor and uncertain events is appropriate. The κ-Cepheids (751 KCE) in September 2015 (Rendtel, 2015) is another similar example.

Table 1 – Visual reports of the October Camelopardalids 2018. All observers listed here were observing from different locations in Germany under good conditions (limiting magnitude between +5.9 and +6.9.)

Observer	Start UT	End UT	Int.	$T_{\rm eff}$ (h)	OCT
Ina Rendtel	18:00	20:05	2	2.00	3
Christoph Gerber	21:43	00:02	5	2.20	2
Roland Winkler	22:05	00:15	2	2.11	2
André Knöfel	22:44	02:45	3	3.49	5
Ina Rendtel	22:57	03:30	18	4.55	21
Jürgen Rendtel	23:00	03:15	15	4.05	16
Sirko Molau	00:20	01:30	1	1.17	0
Kai Schultze	01:12	02:40	2	1.42	6

As a consequence of the low activity level and the short duration of the event, all individual samples are very small. The four video cameras working from one location (Ketzür, west of Potsdam, Germany) show flux density values which differ from each other by a factor of 10! The cameras heading to the east and south (Remo1 and Remo2) recorded 13 and 14 OCT, respectively. This corresponds to a flux density of about $2/(1000\ \mathrm{km^2 h})$. Remo3 and Remo4, looking north and west, recorded only 2 OCT each, yielding a flux density of $0.2/(1000\ \mathrm{km^2 h})$. All cameras had identical field sizes and about the same limiting magnitude and recorded in total between 105 and 138 meteors each. Similar effects due to the small numbers may have affected the visual data (see Table 1).

3 Results and Discussion

Activity of the October Camelopardalids (OCT) was detectable for about five hours as shown in Figure 1 and reached a maximum ZHR ≈ 5 using a population index $r = 2.5$ and a minimum interval length of 1 hour. Due to the small number of OCT meteors, all four ZHR values shown are based on 8–12 meteors only. Seen also the comments above, the agreement of both profiles is remarkable. There is a third independent data set from radio forward scatter data shown

[1]Leibniz-Institut für Astrophysik, An der Sternwarte 16, 14480 Potsdam and International Meteor Organization, Eschenweg 16, 14476 Potsdam, Germany. Email: jrendtel@web.de

[2]Abenstalstr. 13b, 84072 Seysdorf, Germany. Email: sirko@molau.de

IMO bibcode WGN-465-rendtel-oct
NASA-ADS bibcode 2018JIMO...46..173R

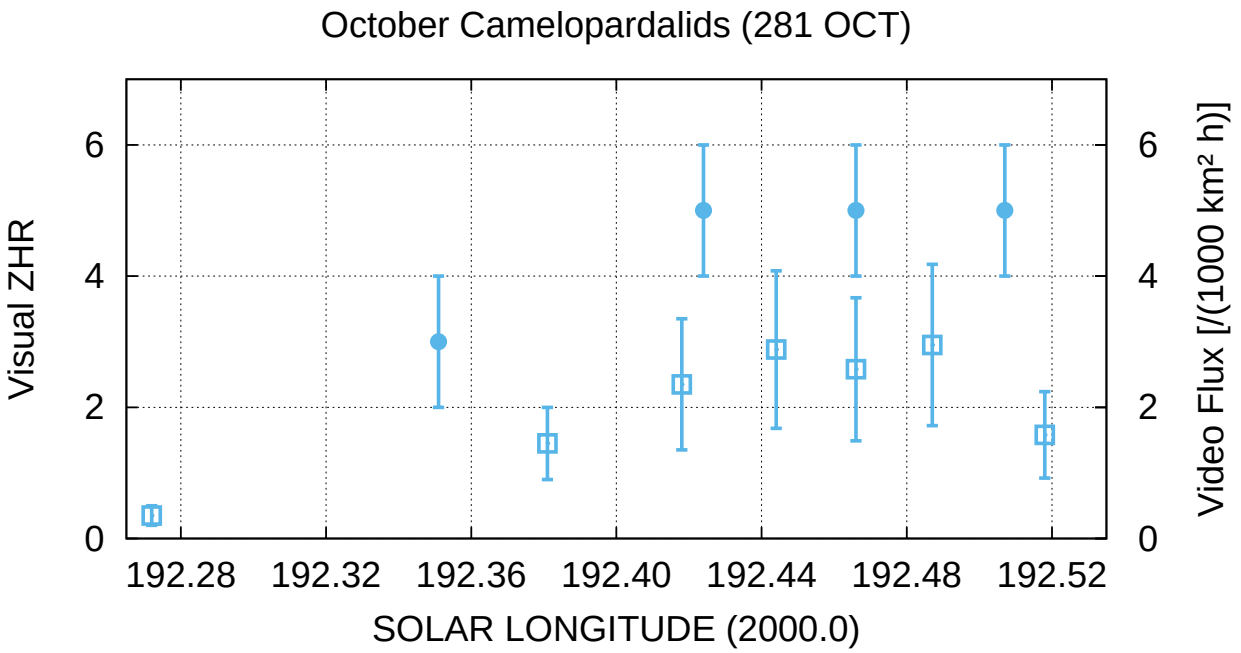

Figure 1 – Visual ZHR (dots) and video meteor flux density (open squares) of the October Camelopardalids during the night 2018 October 5/6. The abscissa steps are equivalent to 1 hour.

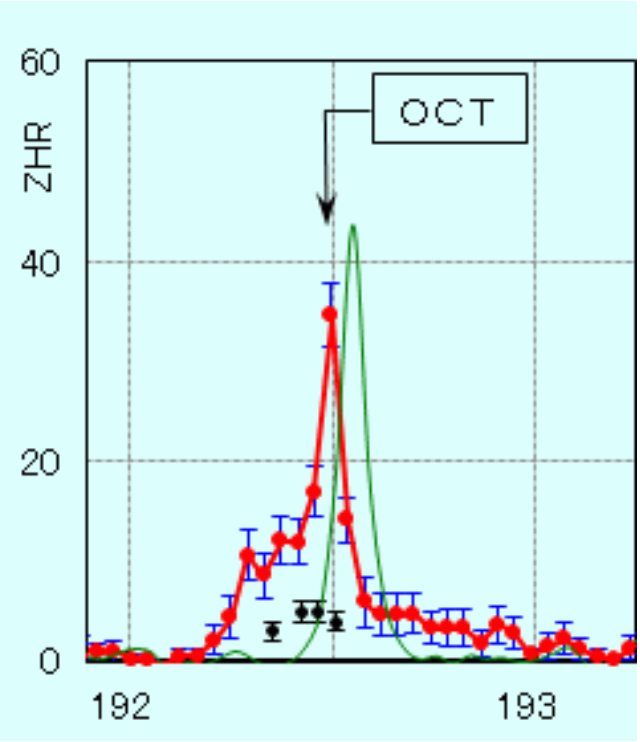

Figure 2 – Radio-ZHR of the October Camelopardalids as shown on Hirofumi Sugimoto's web page about radio meteor data (see text).

at `http://www5f.biglobe.ne.jp/~hro/Flash/2018/OCT/index.html` and extracted here as Figure 2 and shows a sharp activity peak at the same position as well. Like in earlier cases, the ZHR value seems to be significantly overestimated – or the shower had a considerable component of weak meteors which were not detected by visual and video observations.

The attempt to locate the centre or peak from a profile with higher temporal resolution brings us right to the end of the possibilities. Figure 3 shows the result with a minimum required bin length of 8 minutes. Each (except 2) ZHR value is based on just four OCT, and probably see only statistical scatter. However, the two intervals with a ZHR of about 8 near 192.°50 are closer to the predicted time than the centre of the smooth profiles shown in Figure 1. Of course, none of the peaks in Figure 3 has a high significance.

We may summarize that the OCT reached a maximum ZHR between 5 (general profile, Figure 1) and perhaps about 10 in two intervals (Figure 3).

The results shown here represent a preliminary analysis to document the event which for the first time was recorded also visually. Our intention is to draw the observers' attention to such minor events which may be easily lost or forgotten if no alert is sent out and later no response is given.

The calculated peak time for 2018 was October 6, $02^{h}17^{m}$ UT ($\lambda_{\odot} = 192.°529$). The highest observed ZHR and flux density are centered near $00^{h}30^{m}$ UT with an uncertainty of about 1.3 hours ($\lambda_{\odot} = 192.°45 \pm 0.°05$) and thus occurred almost two hours earlier.

The next possible OCT return is calculated for 2019 at the same position. Seen the uncertainty of the maximum timing in 2018, the 2019 shower might occur slightly earlier, too. Observers should be alerted not only near 2019 October 6 $08^{h}25^{m}$ UT but also before this time.

The recent observations confirm the statement given for the 2018 prediction, that surprises are possible. Esko Lyytinen commented his modelling results with the remark that the stream is quite reliably a long-period case with an untypical wide 1-revolution trail – or we have not yet encountered the densest part of the trail.

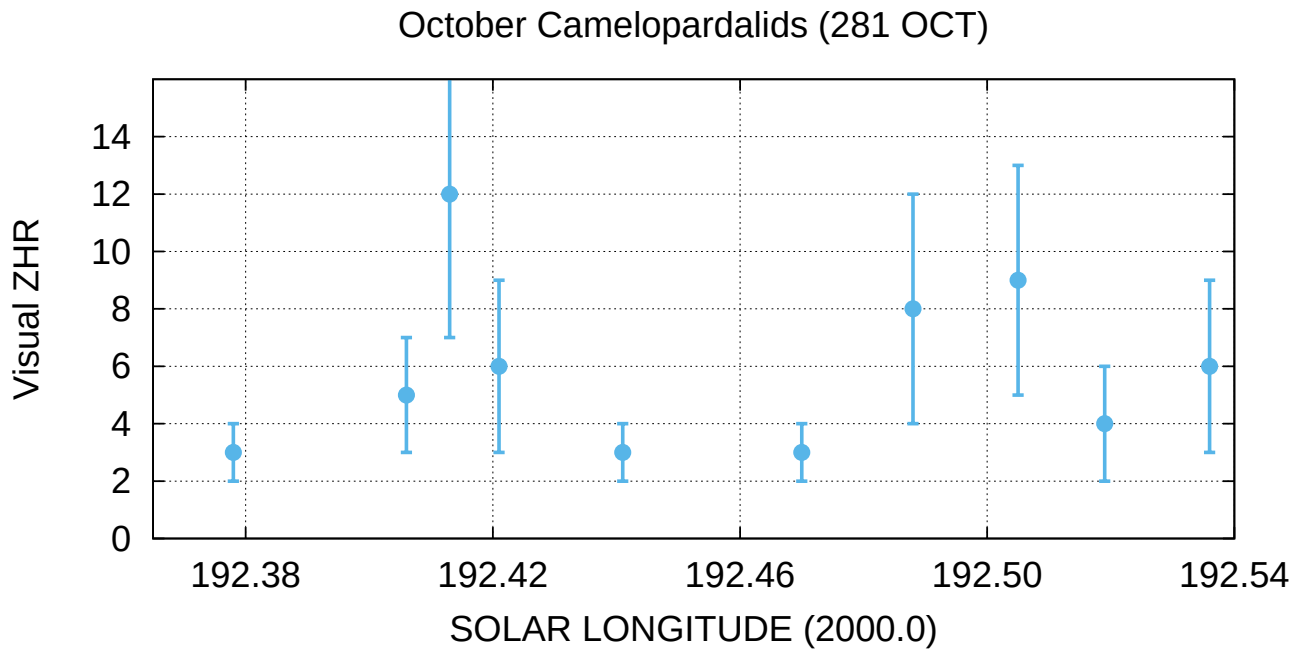

Figure 3 – Attempt to reach a higher temporal resolution form the visual data ($0^\circ.04$ are approximately 1 hour). Here the individual ZHR values represent bins with just four meteors (except the values at $192^\circ.413$ and $192^\circ.470$ with six OCT each), but considering only ZHR values based on at least two count intervals. However, the apparent peaks may easily be artefacts.

References

Molau S., Crivello S., Goncalves R., Saraiva C., Stomeo E., and Kac J. (2017). "Results of the IMO Video Meteor Network – October 2016". *WGN, Journal of the IMO*, **45**, 39–42.

Rendtel J. (2015). "Minor kappa-Cepheid (751 KCE) activity on 2015 September 21". *WGN, Journal of the IMO*, **43**, 177–178.

Rendtel J. (2017). "Meteor Shower Calendar 2018". International Meteor Organization. IMO_INFO(2-17).

Rendtel J., Ogawa H., and Sugimoto H. (2017). "Meteor showers 2016: review of predictions and observations". *WGN, Journal of the IMO*, **43**, 49–55.

Handling Editor: Javor Kac
This paper has been typeset from a LaTeX file prepared by the authors.

History

A History of Meteor Reports in The Astronomer magazine: part 2 1975–1989

Tracie Heywood[1]

The magazine "The Astronomer" is a monthly magazine published in the UK whose aim is the rapid publication of observations made by amateur astronomers. It was first published in 1964. This is the second article in a series that provide an overview of the magazine's meteor content and covers the years 1975–1989.

Received 2018 July 30

1 Editorial and Sub-Editorial Changes

1975 sees a change of Editor for the magazine, with James Muirden producing his final issue in March of that year. Guy Hurst takes on the role of Editor as from the April issue.

This period also sees two changes of Meteor sub-editor. Graham Winstanley steps down from the role in February 1976, with Colin Henshaw taking on the role from April onwards. Colin Henshaw steps down at the start of September 1980, with Tony Markham taking over as from the November issue.

The Meteor Notes column now appears on a regular basis. Most reports cover meteor watches carried out near the maxima of the major showers. The Perseids prove particularly popular and such is the volume of contributions that it is often necessary to spread reports over more than one issue of the magazine. Some contributions, however, look at other aspects of meteor observing.

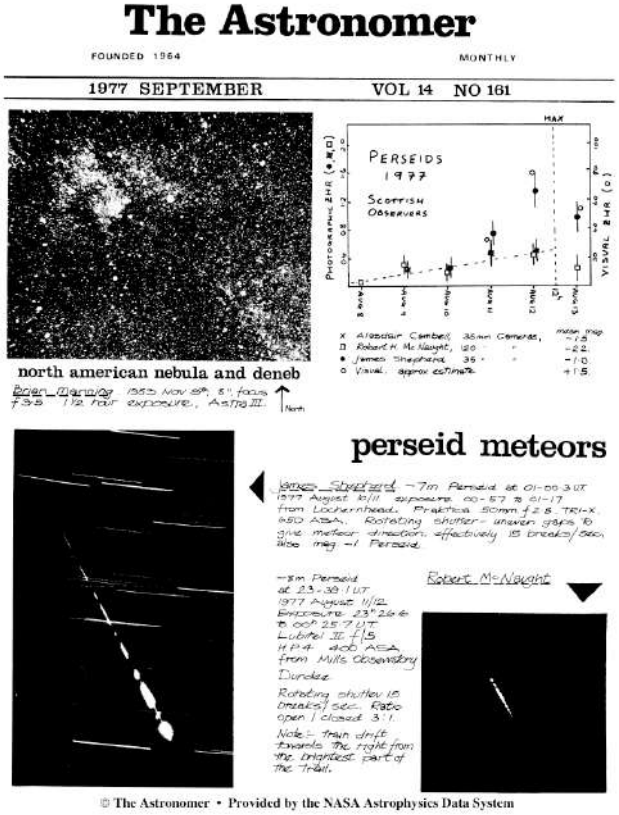

Figure 1 – September 1977 issue cover.

2 "Optical Delusions"

In the 1976 June issue (Craven, 1976b), Jim Craven describes examples of spurious meteors that he has noted during meteor watches:

Since starting serious meteor observations about 18 months ago, I have noticed several optical delusions that regularly recur during naked-eye sessions . . .

1. *The "Black Meteor" – a short sudden movement of a steak of sky, blacker than the background, thus giving the impression of a black meteor.*

2. *Shortish, fast "meteors", always faint, about 1 mag above the prevailing Lim Mag. These are discounted because they usually occur when changing the center of the field of view.*

3. *Faint, fast "meteors" with paths directly between 2 adjacent stars up to 10 degrees apart. Usually off center of field. Clearly some meteors must pass through two bright stars, but this is seen far too often to be acceptable.*

4. *Short, faint meteors, mag 3 or 4, apparently stemming from a star, usually off center of the field of view and seen even when my head is still. Again, it must really occur sometimes, but not as often.*

5. *Sudden brightening of a bright star by two or three mags. Again, off center of the field of view and, once noticed, will recur with the same star throughout the session.*

(Alastair McBeath later comments on these and other unusual phenomena in a paper (McBeath, 1996) presented to the IMO Conference in 1995, linking some of these phenomena to the creation of artificial linear sources from noise in the eye-brain system)

3 Meteor Sounds

The issue of meteor sounds briefly resurfaces in the mid-1970s. In the 1976 March issue (Paine, 1976), Alan

[1]20 Hillside Drive, Leek, ST13 8JQ, UK.
Email: tracieheywood832@gmail.com

IMO bibcode WGN-465-heywood-ta2
NASA-ADS bibcode 2018JIMO...46..176H

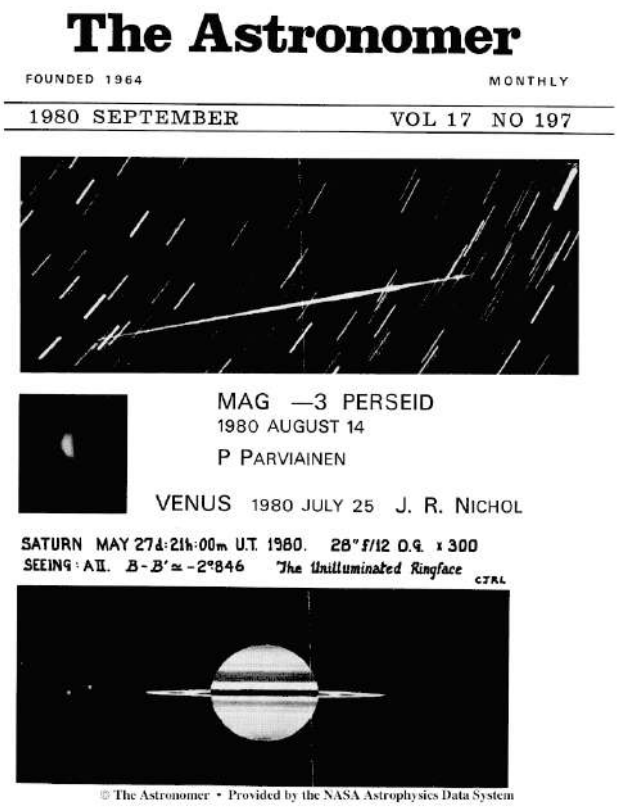

Figure 2 – September 1980 issue cover.

Paine quotes two occasions on which he has heard simultaneous sounds. In the 1976 April issue (Botley & Sewell, 1976), Cicely M Botley mentions some historical reports of meteor sounds and adds *"It is also likely that as with sounds from the aurora, hearing depends on personal sensitivity"*. In the same issue, David Sewell speculates that the occurrence of sounds may be related to the amount of metal content present and suggests that the "swishing" sound sometimes reported may relate to the generation of steam.

A longer discussion starts in late 1979. Following Dave Powell's report in the 1979 September issue (Powell, 1979) of a "swishing sound" coincident with a mag −1 Perseid and David Storey's report in the 1979 November issue (Storey & Henshaw, 1979) of hearing a "fizz" from two other meteors, Colin Henshaw responds *"I find it amazing that some observers still claim they can hear meteors. . . "*. Alan Paine responds at length in the 1979 December (Paine & Henshaw, 1979) and 1980 January issues (Paine & Bone, 1980). He favours the (somewhat vague) idea that the sound is being generated locally via energy received electromagnetically from the meteor. In the latter issue, Neil Bone supports the sub-editor and suggests that reports of meteor sounds are due to people *"taking the analogy between fireworks and meteors a bit too far"*. Further comments by David Storey, Alan Paine and Tony Tanti appear in the 1980 March issue (Paine et al., 1980) and in the 1980 April issue (Storey, 1980).

4 Perseid subcenters?

In his preview of forthcoming events in the 1976 July issue (Henshaw, 1976), Colin Henshaw mentions that the Soviet observer Martynenko has published a chart showing four subcenters of the Perseid radiant. These are located at:

1) 2^h25^m +57d 2) 3^h00^m +55d
3) 3^h05^m +41d 4) 3^h15^m +49d

No reference is quoted, although the source may be the same as those (Martynenko & Smirnov, 1973; Martynenko et al., 1973) quoted by Gary W Kronk in his 1988 book "Meteor Showers: A Descriptive catalog":

In the 1976 September issue (Craven, 1976a), Jim Craven reports his monitoring of activity from these four subcenters, finding that of the 50 Perseids he was able to allocate, almost half came from subcenter 1, with the remainder being more evenly split between the other three. He also proposes the existence of a fifth subcenter near RA 01^h30^m, +58d.

(2018 note: The claims for the existence of these Perseid subcenters seem to have been based on visual observations only. These subcenter claims do not appear to have "survived" into the era of video imaging. Possibly we were seeing a tendency of the eye, when tracing meteor paths backwards, to "gravitate" towards bright stars. The five proposed subcenters were close to the double cluster, gamma Per, alpha Per, beta Per and delta Cas).

5 Minor Shower knowledge

Colin Henshaw's previews of forthcoming events also give an insight as to the understanding (or, it is probably more accurate to say, confusion) in the 1970s regarding minor meteor showers. Here, for example, is the content from the 1976 July issue:

"The Kappa Cygnids, renowned for their exploding fireballs, are favourably placed this year. They are active between Aug 19-22 but only a low max of 4 meteors per hour is expected on Aug 20/21. The Epsilon Lyrids are active between Aug 10-20 and were discovered by Soviet amateurs stationed in the Crimea. Nothing is known so far on rates. Old editions of Norton's list several minor showers as being active during Aug. The Alpha Cygnids and Lacertids are still continuing from July and the Alpha Aurigids start on Aug 12. This latter shower is described by Norton's as yielding "swift" meteors. Hungarian obs in 1973 have shown the existence of several radiants around Capella in the beginning of Aug, yielding rates as high as 16 meteors per hour. The Omicron Draconids, displaying slow meteors, are listed as being active during Aug 21-23. The Zeta Draconids also yield slow meteors and are active between Aug 21-31."

(2018 note: With the exception of the Kappa Cygnids, none of the above meteor shower activity is listed in the 2018 IMO Meteor Shower calendar or in the IAU's list of established meteor showers. It is also unlikely that any of the other showers appear in the IAU's working list of meteor showers under a different name.

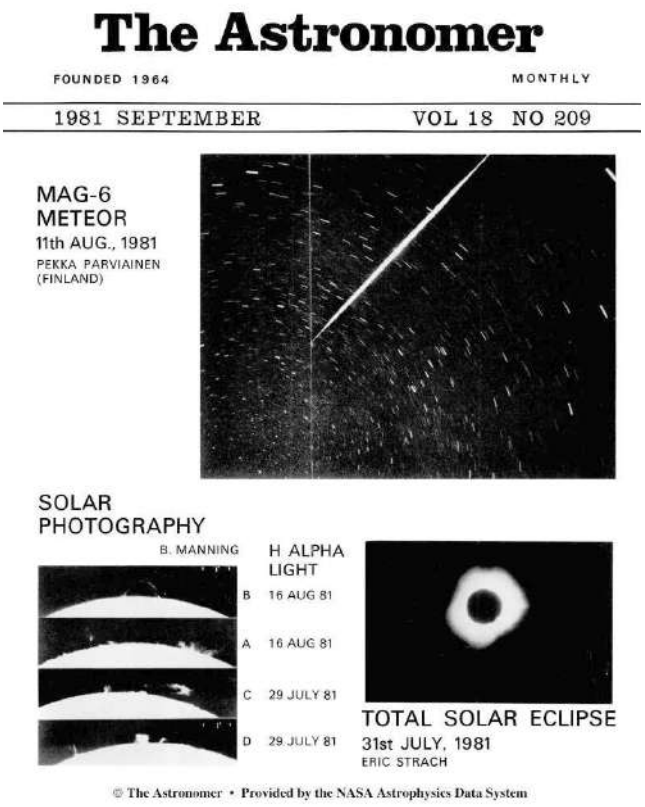

Figure 3 – September 1981 issue cover.

There is a quite high probability that the meteors assigned to the Alpha Aurigids around August 12 and to other radiants near Capella in early August were merely mis-identified visually observed Perseids).

6 1980 Perseids

Comet Swift-Tuttle 1862 III, the parent comet of the Perseids had last passed through perihelion in 1862. The orbital period of the comet was believed to be around 120 years and thus it was generally assumed that the next perihelion passage would take place in 1981, give or take a year. It was also expected that this would lead to an enhancement in Perseid rates. Hopes increased as Perseid peak ZHRs appeared to be increasing during the late 1970s. Outlining the BAA Meteor Section's plans for the 1980 Perseids in the 1980 July issue (Spalding, 1980), George Spalding offers this incentive:

"The parent comet, 1862 III Swift-Tuttle will return to perihelion in a year or two and rates may be enhanced in the next few years"

It was somewhat unfortunate timing in that, a short time later, TA found itself without a Meteor sub-editor and thus most reports of the 1980 Perseids are not published until the October issue (The Astronomer, 1980a) and the November issue (The Astronomer, 1980b). These show that observers of the 1980 Perseids had certainly not been disappointed, having witnessed Perseids rates that were considerably enhanced.

(Although some authors would later cast doubt on these enhanced rates, it is now generally accepted that rates were significantly enhanced in 1980, but the enhancement was related to the 12-year resonance in Perseid rates caused by Jupiter, rather than being due to the proximity of the Perseid parent comet, which, we later discover, does not reappear for another decade.)

7 1982 Lyrid outburst

The short-lived outburst from the Lyrids during the morning of 1982 April 22 occurs too late to be seen from European longitudes, but Paul Jones and Brenda Branchett, in Florida, are better placed. In the 1982 June issue (Jones, 1982), Paul reports seeing Lyrid rates rising from just 12 in the previous hour to a peak of 74 Lyrids in the hour from $04^{h}25^{m}$ to $05^{h}25^{m}$ UT and then dropping to a "mere" 43 an hour later (LM 6.5). Jonathan Shanklin, returning by sea after five months working in the Antarctic, also sees the Lyrid activity, reporting his observations in the 1982 July issue (Shanklin, 1982). He is at a more southerly and thus less favorable location (Lat 28 S, Long 26 W) and has cloud interference at the time of the peak, but still manages to see 35 Lyrids and 5 sporadics in clearer skies between $06^{h}13^{m}$ and $07^{h}10^{m}$ UT.

8 Photographic Imaging

Although naked-eye visual meteor observing dominates, there is also some meteor imaging, based around long exposures, typically of 10-15 minutes (longer if sky darkness permits), with camera systems often being fitted with rotating shutters.

In the 1978 March issue (McNaught, 1978), Robert McNaught summarizes his photographic results from 1977. Operating eight Lubitel 2 cameras, he had captured images of 30 meteors, amounting to a capture rate of one sporadic being imaged for every 40.8 camera hours. The most impressive events had been a mag −8 Perseid during the night of 1977 Aug 11-12 and a mag −12 sporadic on during the night of 1977 Sep 16-17. Impressive fireball images also appear on a good number of other TA covers. These include James Shepherd's image of a mag −7 Perseid (1977 September, (Shepherd, 1977), Figure 1), Pekka Parviainen's image of a mag −6 fireball (1981 September, (Parviainen, 1981), Figure 4), Roberto Haver's image of a mag −13 fireball (1982 August, (Haver, 1982)) and Robert McNaught's image of a mag −10 fireball (1983 September, (McNaught, 1983a), Figure 3).

BAA Meteor Section plans for Meteor Triangulation work during the New Moon weekends of August and September are described by Robert McNaught in the 1982 August issue (McNaught, 1982a). He also reports the analysis of a 3-station capture from July.

Articles about meteor photography appear in two issues from 1985. In an article in the March issue (Bone, 1985), Neil Bone expresses a preference for wide-angle lenses over faster lenses, finding that the former produce a higher capture rate. This encourages Steve Evans to write an article for the June issue (Evans, 1985) in which he describes additional factors that influence the capture rate.

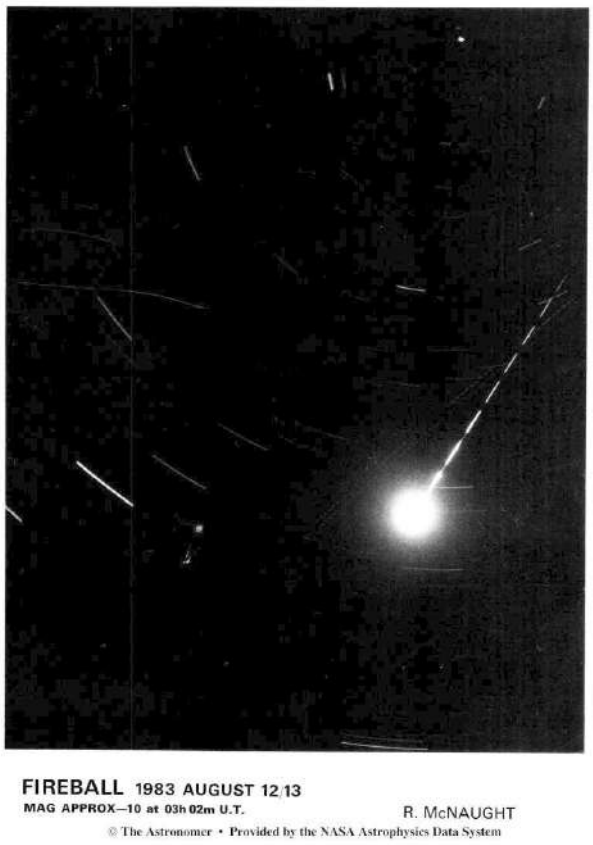

Figure 4 – September 1983 issue back cover.

9 Video imaging

The first video images appear in TA during 1982 and feature the planets and lunar craters. Video imaging of meteors makes its debut in the 1983 October issue (McNaught, 1983b) when Robert McNaught describes the results he obtained during the 1983 Perseids having loaned a low light level TV camera from the University of Southampton. Around 100 meteors, around 90% being Perseids, are recorded during the night of Aug 12-13 and fifteen of these are subsequently shown on the national TV news. There is, of course, no way to include these videos in TA. Later in the 1980s, a number of meteor video clips are shown during the annual TA AGM meetings.

10 Meteor or Satellite?

One of the challenges posed by meteor imaging concerns making a decision as to whether a "streak of light" recorded on a still image is that of a meteor or is of some other object, such as an aircraft or a satellite. This is especially true when the area of sky involved was not being monitored visually.

In late 1983 and 1984 we see a lengthy discussion regarding an image captured by John Burger during an exposure lasting from $00^{h}05^{m} - 00^{h}26^{m}$ UT on 1983 August 13 and published in the 1983 November issue (Burger, 1983). The object is initially described as a Perseid, but in the December issue (Eberst, 1983), Russell Eberst suggests that it actually shows the classified American surveillance satellite 82-111A, rather than a meteor. By chance, the same object had been imaged by Noel White during an exposure lasting from $00^{h}21^{m} - 00^{h}40^{m}$ UT and this image appears in the January issue (White, 1984a). In the 1984 March issue (White, 1984b), it is reported that Roy Panther had used triangulation to calculate the position of the satellite at the time of a bright spot in the trail present in both images. This is found to have occurred above the town of Beverley in East Yorkshire, at an altitude of 225 miles (362 km). A third image, accompanied by a visual sighting then comes to light in the 1984 April issue (Cooper, 1984), with J Cooper revealing that he saw the object visually at $00^{h}23^{m}$ UT, noting that the bright spot in the image coincided with it brightening to mag −4. He suggests Big Bird (Operations 9627) as an alternative satellite identification.

The 1988 October issue (James, 1988) includes a photograph taken by Nick James that appears to show four parallel meteor trails. Russell Eberst responds in the November issue (Eberst, 1988), revealing that image actually shows four of the six 'whitecloud' secret USA satellites that were orbiting in formation.

11 Upper Atmosphere or More Distant?

Another consideration involves whether meteor observers might by chance record other astronomical phenomena during their meteor watches. One early 20^{th} century example had been Nova (DQ) Herculis which was discovered by meteor observer J P M Prentice during a Geminid meteor watch in the early hours of 1934 December 12.

Two items submitted by Robert McNaught consider other possibilities:

The first is an article titled "Meteor Observing and Flare Stars" in the 1979 August issue (McNaught, 1979). In this article he suggests that telescopic meteor observers might choose fields of view that contain the locations of known flare stars. He also suggests that meteor imagers check their photographs for any short trails at the positions of known flare stars.

The second item appears in the 1982 March issue (McNaught, 1982b) and appears to simply be a request from the BAA Meteor Section for observers to report the positions of any stationary meteors that they had seen in earlier years. In reality, this request is related to Gamma Ray Bursts. At that time, the nature of GRBs was unknown. It had been suggested that they might also produce optical flashes and/or be recurrent. It was possible that some of the events recorded as stationary meteors could have been such optical flashes and thus the compilation of a list of stationary meteor positions might prove useful as it could be compared with the positions of historical and future GRBs.

(We now, of course, know that GRBs are one-off events. They do produce optical flashes but almost all peak well below the naked-eye limiting magnitude.)

12 Mystery objects

Fewer mystery objects are report in TA during this period than during the magazine's first decade.

In the 1978 July issue (Arbour, 1978), Ron Arbour reports seeing a 2nd magnitude blue-white stellar object in the Ursa Major area that remained visible for about 10 seconds. The 1980 May issue (Sturdy, 1980) includes a report from Keith Sturdy of a 2nd magnitude star-like object surrounded by a nebulous glow that slowly moved from Perseus to Cepheus over a 12 second interval. An additional report of this object by D Roos appears in the 1980 July issue (Roos, 1980).

In the 1987 March issue (Hill, 1987), Harold Hill reports seeing a bright object near the Moon that moved in a SSE direction over a 12 minute interval. Inspection using a telescope showed it to consist of a brighter central object surrounded by several "appendages". Geoffrey Falworth responds in the May issue (Falworth & Hill, 1987) and suggests that the "object" was most likely a group of migrating geese.

13 LM estimation

BAA Meteor Section Circular 28, issued in July 1988, had encouraged observers to try out an alternative method for estimating the limiting magnitude. This involved counting the number of stars visible within certain triangles, defined by bright stars. In the 1988 September issue (Markham, 1988), Tony Markham reports his experience in using this method during the 1988 Perseids. His conclusion is that the triangle-based method tends to underestimate the limiting magnitude, sometimes by more than half a magnitude, compared with methods that are based around looking for specific stars. In the triangle-based method, faint stars are often missed, especially if they were close to other stars. Triangles that feature a Milky Way background fare particularly poorly.

14 Looking Beyond the Visual

Not surprisingly, almost all meteor reports during these years relate to visible light, with only a few venturing beyond this.

In the 1988 February issue (Hartridge & Buckman, 1988), Andrew Hartridge and Alan Buckman report their radio observations of the 1988 Quadrantids. This had involved using a purpose-built Yagi aerial to monitor reflections of the signal from Radio Gdansk at 70.31 MHz.

The 1988 September issue (Oates, 1988) includes a photograph of a Perseid imaged by Michael Oates using infrared film. Michael takes things a step further the following year with the 1989 September issue (Oates, 1989b) including two of his photographs, both of which show the same Perseid meteor. One shows it in white light; the other shows the image captured using infrared film. In the accompanying notes (Oates, 1989a), he highlights the differences between the two images with the infrared image showing little of the flaring present in the white light image.

15 In Conclusion

The late 1970s has been an exciting time for meteor observers who were anticipating the return of the Perseid parent comet Swift-Tuttle 1862 III around 1981. This never happened. Many observers assumed that it had passed through perihelion unseen and that the high ZHR of 1980 Perseid had been related to its return. A few observers, however, held on to a suggestion that the comet might return as late as 1992. In the 1989 May (Mobberley, 1989) issue, Martin Mobberley provides a month-by-month list of potential recovery coordinates.

In the aftermath of the Swift-Tuttle "no show", the 1980s were a challenging time for meteor observers with light pollution issues spreading beyond urban areas and into semi-rural areas. This was having an effect not just on the number of meteor watches carried out but also, more significantly, on the number of new people taking up meteor observing.

On a more positive note, as the 1980s came to an end, we were only a decade or so away from a possible Leonid meteor storm.

References

Arbour R. (1978). "A flare object in Ursa Major?". *The Astronomer*, **15:171**, 56.

Bone N. M. (1985). "Some aspects of meteor photography". *The Astronomer*, **21:251**, 189–190. [11:189-11:190].

Botley C. M. and Sewell D. (1976). "Meteoritic sounds". *The Astronomer*, **12:144**, 244.

Burger J. A. (1983). "Perseid 1983 Aug 12/13". *The Astronomer*, **20:235**, C1. [Cover 7:1].

Cooper J. (1984). "Burger's object of 1983 Aug 12/13". *The Astronomer*, **20:240**, 212,214. [12:212,12:214].

Craven J. (1976a). "Meteor Notes". *The Astronomer*, **13:149**, 98. [5:98].

Craven J. (1976b). "Optical delusions". *The Astronomer*, **13:146**, 32. [2:32].

Eberst R. D. (1983). "November cover comments". *The Astronomer*, **20:236**, 121–122. [8:121-8:122].

Eberst R. D. (1988). "Satellites". *The Astronomer*, **25:295**, 148. [7:148].

Evans S. (1985). "In praise of the Lubitel, some more aspects of meteor photography". *The Astronomer*, **22:254**, 21–22. [2:21-2:22].

Falworth G. and Hill H. (1987). "Unusual object near the Moon, 1987 Mar 8". *The Astronomer*, **24:277**, 130–131. [1:10-1:11].

Hartridge A. and Buckman A. (1988). "Meteor radio echoes". *The Astronomer*, **24:286**, 200. [10:200].

Haver R. (1982). "Mag -13 fireball". *The Astronomer*, **20:220**, C3. [Cover 13:Z1].

Henshaw C. (1976). "Forthcoming events". *The Astronomer*, **13:147**, 48. [3:48].

Hill H. (1987). "Unusual object near the Moon, 1987 Mar 8". *The Astronomer*, **23:275**, 178. [11:178].

James N. D. (1988). "Four parallel meteor trails?". *The Astronomer*, **25:294**, C3. [Cover 12:Z1].

Jones P. (1982). "The 1982 Lyrid meteor shower". *The Astronomer*, **19:218**, 24–25. [2:24-2:25].

Markham T. (1988). "Limiting magnitudes". *The Astronomer*, **25:293**, 94. [5:94].

Martynenko V. V. and Smirnov N. V. (1973). "The structure of the Perseids radiants in 1971". *Solar System Research*, **7**, 104–109.

Martynenko V. V., Vagner L. Ya., and Levina A. S. (1973). "Comparison of activity of Perseids in 1970 and 1971". *Solar System Research*, **7**, 163–165.

McBeath A. (1996). "Unusual meteor observations". In *Proceedings IMC Brandenburg 1995*. pages 118–122.

McNaught R. H. (1978). "Meteor photography using Lubitel 2 cameras in 1977". *The Astronomer*, **14:167**, 205–206. [11:205-11:206].

McNaught R. H. (1979). "Meteor observing and flare stars". *The Astronomer*, **16:184**, 80–81.

McNaught R. H. (1982a). "Meteor triangulation". *The Astronomer*, **19:220**, 72–73. [5:72-5:73].

McNaught R. H. (1982b). "Stationary meteors". *The Astronomer*, **18:215**, 238. [11:238].

McNaught R. H. (1983a). "Fireball 1983 August 12/13". *The Astronomer*, **20:233**, C4. [Cover 12:Z2].

McNaught R. H. (1983b). "Video results". *The Astronomer*, **20:234**, 91. [6:91].

Mobberley M. (1989). "Recovering Swift-Tuttle from the northern hemisphere". *The Astronomer*, **26:301**, 5–6. [1:5-1:6].

Oates M. (1988). "Perseid meteor with infrared film: 1988 Aug 13". *The Astronomer*, **25:293**, C1. [Cover 5:1].

Oates M. (1989a). "Cover notes". *The Astronomer*, **26:305**, 102. [5:102].

Oates M. (1989b). "Perseid meteor, 1989 Aug 12". *The Astronomer*, **26:305**, C3. [Cover 13:Z1].

Paine A. (1976). "Meteoritic sounds". *The Astronomer*, **12:143**, 225–226.

Paine A. and Bone N. M. (1980). "Meteor Notes". *The Astronomer*, **16:189**, 180–181. [9:180-9:181].

Paine A. and Henshaw C. (1979). "Meteor Notes". *The Astronomer*, **16:188**, 164–166. [8:164-8:166].

Paine A., Storey D., and Tanti T. (1980). "Meteor Notes". *The Astronomer*, **16:191**, 227–228. [11:227-11:228].

Parviainen P. (1981). "Mag -6 meteor, 11th Aug 1981". *The Astronomer*, **18:209**, C1. [Cover 5:1].

Powell D. (1979). "Meteor Notes". *The Astronomer*, **16:185**, 97. [5:97].

Roos D. (1980). "Unidentified object (Sturdy)". *The Astronomer*, **17:195**, 61. [2:61].

Shanklin J. D. (1982). "Astronomy in the Southern Ocean". *The Astronomer*, **19:219**, 53–54. [3:53-3:54].

Shepherd J. (1977). "Perseid meteors". *The Astronomer*, **14:161**, C1. [Cover 5:C1].

Spalding G. (1980). "BAA.MS coverage of the Perseids, 1980". *The Astronomer*, **17:195**, 51. [2:51].

Storey D. (1980). "Meteor Notes". *The Astronomer*, **16:192**, 245–246. [12:245-12:246].

Storey D. and Henshaw C. (1979). "Meteor Notes". *The Astronomer*, **16:187**, 143. [7:143].

Sturdy K. (1980). "Unidentified object". *The Astronomer*, **17:193**, 14. [1:14].

The Astronomer (1980a). "Meteor Notes". *The Astronomer*, **17:198**, 117–118. [10:435-10:436].

The Astronomer (1980b). "Meteor Notes". *The Astronomer*, **17:199**, 132–134. [11:575-11:577].

White N. (1984a). "82-111a Burger's meteor 1983 Aug 12/13". *The Astronomer*, **20:237**, C4. [Cover 12:Z2].

White N. (1984b). "Burger's object of 1983 Aug 12/13". *The Astronomer*, **20:239**, 173. [11:173].

Back issues of most issues of the magazine have been uploaded to the NASA ADS system and can be downloaded via this link on the magazine's home page: `http://www.theastronomer.org/post/NASA%20ADS/`

Unfortunately, the page-ids stored in the NASA ADS system don't always directly match the page numbers from the printed magazine. To help mitigate this problem, those page-ids that differ from the printed values have been included (when available) in brackets at the end of each reference.

Handling Editor: Javor Kac

The International Meteor Organization

www.imo.net

Follow us on Facebook InternationalMeteorOrganization

Follow us on Twitter @IMOMeteors

Council

President: Cis Verbeeck,
Bogaertsheide 5, 2560 Kessel, Belgium.
e-mail: cis.verbeeck@scarlet.be

Vice-President: Juraj Tóth,
Fac. Math., Phys. & Inf., Comenius Univ.,
Mlynska dolina, 84248 Bratislava, Slovakia.
e-mail: toth@fmph.uniba.sk

Secretary-General: Robert Lunsford,
14884 Quail Valley Way, El Cajon,
CA 92021-2227, USA. tel. +1 619 755 7791
e-mail: lunro.imo.usa@cox.net

Treasurer: Marc Gyssens, Heerbaan 74,
B-2530 Boechout, Belgium.
e-mail: marc.gyssens@uhasselt.be
BIC: GEBABEBB
IBAN: BE30 0014 7327 5911
Bank transfer costs are always at your expense.

Other Council members:

Megan Argo, Jodrell Bank Centre for Astrophysics,
Alan Turing building, University of Manchester,
Oxford Road, Manchester, M13 9PL, UK.
e-mail: megan.argo@gmail.com

Javor Kac (see details under WGN)

Detlef Koschny, Zeestraat 46,
NL-2211 XH Noordwijkerhout, Netherlands.
e-mail: detlef.koschny@esa.int

Masahiro Koseki, 4-3-5 Annaka, Annaka-shi,
Gunma-ken 379-0116, Japan.
e-mail: geh04301@nifty.ne.jp

Sirko Molau, Abenstalstraße 13b, D-84072 Seysdorf,
Germany. e-mail: sirko@molau.de

Jean-Louis Rault, Société Astronomique de France,
16, rue de la Vallée, 91360 Epinay sur Orge,
France. e-mail: f6agr@orange.fr

Jürgen Rendtel, Eschenweg 16, D-14476 Marquardt,
Germany. e-mail: jrendtel@aip.de

Paul Roggemans, Pijnboomstraat 25, 2800 Mechelen,
Belgium, e-mail: paul.roggemans@gmail.com

Galina Ryabova, Res. Inst. of Appl. Math. & Mech.,
Tomsk State University, Lenin pr. 36, build. 27,
634050 Tomsk, Russian Federation.
e-mail: ryabova@niipmm.tsu.ru

Damir Šegon, J. Rakovca 3, 52100 Pula, Croatia.
e-mail: damir.segon@pu.t-com.hr

Commission Directors

Visual Commission: Rainer Arlt (rarlt@aip.de)
Generic e-mail address: visual@imo.net
Electronic visual report form:
http://www.imo.net/visual/report/electronic

Video Commission: Sirko Molau (video@imo.net)

Photographic Commission: Bill Ward
(William.Ward@glasgow.ac.uk)
Generic e-mail address: photo@imo.net

Radio Commission: Jean-Louis Rault (radio@imo.net)

Fireballs: Online fireball reports:
http://fireballs.imo.net

Outreach Officer

Jure Atanackov, e-mail: jureatanackov@gmail.com

Webmaster

Karl Antier, e-mail: webmaster@imo.net

WGN

Editor-in-chief: Javor Kac
Na Ajdov hrib 24, SI-2310 Slovenska Bistrica,
Slovenia. e-mail: wgn@imo.net;
include METEOR in the e-mail subject line

Editorial board: Ž. Andreić, M. Argo, D.J. Asher,
F. Bettonvil, J. Correira, M. Gyssens,
C. Hergenrother, T. Heywood, J.-L. Rault,
J. Rendtel, C. Verbeeck, S. de Vet, D. Vida.

IMO Sales

Available from the Treasurer or the Electronic Shop on the IMO Website	€	$
IMO membership, including subscription to WGN Vol. 46 (2018)		
Surface mail	26	35
Air Mail (outside Europe only)	49	65
Electronic subscription only	21	25
Proceedings of the International Meteor Conference on paper		
1990, 1991, 1993, 1995, 1996, 1999, 2000, 2002, 2003, per year	9	12
2007, 2010, 2011, per year	15	20
2012, 2013, 2014, 2015 per year	25	34
Proceedings of the Meteor Orbit Determination Workshop 2006	15	20
Radio Meteor School Proceedings 2005	15	20
Handbook for Meteor Observers	15	20
Meteor Shower Workbook	12	16
Electronic media		
Meteor Beliefs Project ZIP archive	6	8

2018 Perseids with Raspberry Pi-based meteor cameras

About 300 meteors recorded with IMX225 camera from Elginfield, Ontario (Canada). Camera operator: Denis Vida (`https://gmn.duckdns.org/`).

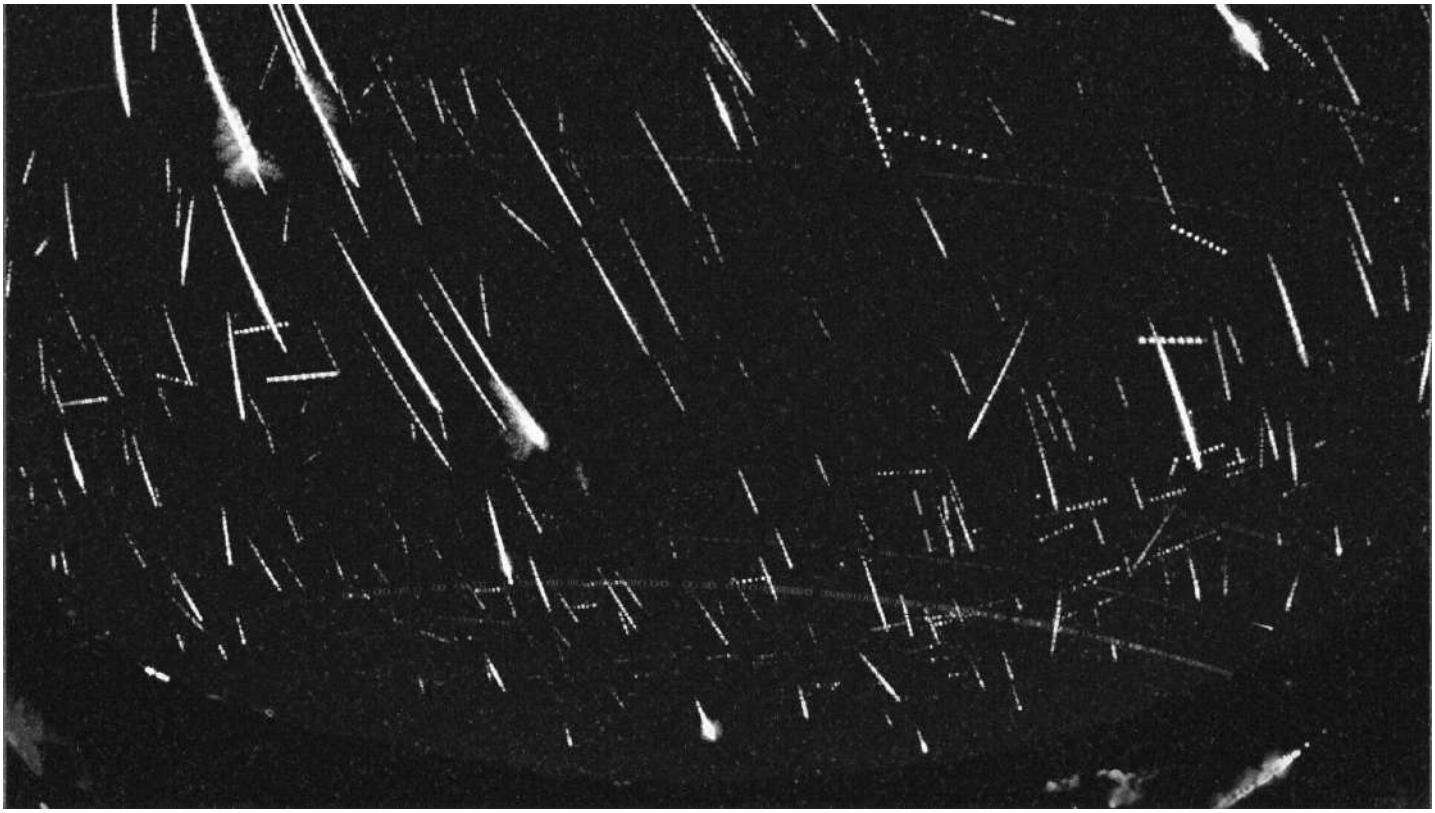

About 300 meteors recorded with Hikvision HD camera from Hum (Istria, Croatia). Camera operator: Aleksandar Merlak (`https://gmn.duckdns.org/`).